IEEE Access
Multidisciplinary ⋮ Rapid Review ⋮ Open Access Journal

Received March 3, 2022, accepted April 4, 2022, date of publication April 11, 2022, date of current version April 22, 2022.

Digital Object Identifier 10.1109/ACCESS.2022.3166241

Non-Terrestrial Networks for UAVs: Base Station Service Provisioning Schemes With Antenna Tilt

SEONGJUN KIM[1], (Student Member, IEEE), MINSU KIM[1], (Student Member, IEEE), JONG YEOL RYU[2], (Member, IEEE), JEMIN LEE[3], (Member, IEEE), AND TONY Q. S. QUEK[4], (Fellow, IEEE)

[1]Department of Electrical Engineering and Computer Science, Daegu Gyeongbuk Institute of Science and Technology, Daegu 42998, South Korea
[2]Department of Information and Communication Engineering, Gyeongsang National University, Tongyeong 53064, South Korea
[3]Department of Electrical and Computer Engineering, Sungkyunkwan University (SKKU), Suwon 16419, South Korea
[4]Information Systems Technology and Design Pillar, Singapore University of Technology and Design, Singapore 487372

Corresponding author: Jemin Lee (jemin.lee@skku.edu)

This work was supported in part by the Institute of Information & communications Technology Planning & Evaluation (IITP) Grant funded by the Korea Government [Ministry of Science and ICT (MSIT)] (Development of 3D Spatial Mobile Communication Technology) under Grant 2021-0-00794; in part by the National Research Foundation of Korea (NRF) Grant funded by the Korea Government [Ministry of Science, ICT and Future Planning (MSIP)] under Grant (NRF-2018R1A5A1060031); in part by the Institute for Information & Communications Technology Promotion (IITP) Grant funded by the Korea Government (MSIP) (Development of Attack Response and Intelligent Road Side Unit (RUS) Technology for Vehicle Security Threat Prevention) under Grant 2021-0-01277; and in part by the National Research Foundation, Singapore, and Infocomm Media Development Authority under its Future Communications Research & Development Programme.

ABSTRACT By focusing on unmanned aerial vehicle (UAV) communications in non-terrestrial networks (NTNs), this paper provides a guideline on the appropriate base station (BS) service provisioning scheme with considering the antenna tilt angle of BSs. Specifically, two service provisioning schemes are considered including the inclusive-service BS (IS-BS) scheme, which makes BSs serve both ground users (GUs) and aerial users (AUs) (i.e., UAVs) simultaneously, and the exclusive-service BS (ES-BS) scheme, which has BSs for GUs and BSs for AUs. By considering the antenna tilt angle-based channel gain, we derive the network outage probability for both IS-BS and ES-BS schemes and show the existence of the optimal tilt angle that minimizes the network outage probability after analyzing the conflict impact of the antenna tilt angle. We also analyze the impact of various network parameters, including the ratio of GUs to total users and densities of total and interfering BSs, on the network outage probability. Finally, we analytically and numerically show in which environments each service provisioning scheme can be superior to the other one.

INDEX TERMS Non-terrestrial network, unmanned aerial vehicle, antenna tilt angle, line-of-sight (LoS) probability, outage probability.

I. INTRODUCTION

Due to the increasing demand for novel and high-quality mobile services, it becomes more difficult to provide reliable communications by the existing terrestrial networks only, up to the level required by future mobile services. To address these issues, non-terrestrial networks (NTNs) have been considered as a promising solution to complement terrestrial networks by providing ubiquitous and global connectivity [1], [2]. Conventional 2D ground space in terrestrial networks is now expanded to 3D aerial space in NTNs with supporting communications for unmanned aerial vehicles (UAVs), high altitude platform systems (HAPS), and satellites [3]. Among them, UAV communications have been in the spotlight because UAVs have more flexible mobility and can locate closer to ground users and base stations (BSs) in terrestrial networks, compared to HAPS and satellites. Therefore, many applications and services based on UAV communications have appeared such as working as a relay in hotspot and a data collector in large-scale networks [4]–[6]. However, the integration of UAVs into existing terrestrial networks brings a lot of challenges such as resource and interference management since UAV communications usually use the frequency band as well as BSs of terrestrial networks.

In this context, many works have been presented for reliable UAV communications. At the beginning of studies, the wireless channel modeling of UAV networks has been

The associate editor coordinating the review of this manuscript and approving it for publication was Emre Koyuncu.

studied in [7]–[10], which is different from that of terrestrial networks. Specifically, according to the height of the UAV, the distance-dependent path loss model for the cellular-to-UAV channel and the line-of-sight (LoS) probability between the UAV and the ground device were modeled in [7], [8] and [9], [10], respectively.

Based on the wireless channel modeling of UAV networks, the optimal location of UAVs for various environments and applications were studied in [11]–[18]. The deployment and the power allocation for the UAV were jointly optimized to minimize the outage probability in [11], [12]. The UAV height and the antenna beamwidth were jointly optimized to maximize the data rate [13] and the coverage probability [14]. The joint optimization of the UAV trajectory and the spectrum allocation was considered to maximize the throughput [15] and minimize the mission completion time [16]. The outage probability was presented by considering the effect of the UAV height and the channel environment in [17]. In [18], multi-layer aerial networks were considered and designed optimally to maximize the successful transmission probability and the area spectral efficiency. However, the works in [12], [13], [15], [16] made a strict assumption that UAV-to-ground communications channels are dominated by LoS links only without considering the location-dependent probability of having LoS links. Furthermore, all those aforementioned works did not consider a BS antenna tilt angle, which significantly affects the communication performance between the ground BS and the UAV. Especially, the antenna tilt angle of the ground BS has been conventionally designed for ground devices only, so the UAV can receive the signal from these BSs with considerably small power [19], [20].

To overcome these issues, the efficient design of the BS antenna tilt angle for UAV communications has been considered in recent works [21]–[27]. The vertical antenna gain was considered for analyzing the successful transmission probability of UAV communications in [21]. The BS antenna tilt angle was optimized to maximize the coverage probability according to the heights of the UAV and the BS in [22], [23], and also to maximize the successful content delivery probability in massive multiple-input multiple-output (MIMO) systems in [24]. The BS association probability and signal-to-interference-plus-noise ratios (SINRs) were studied for two different association policies such as nearest-distance based and maximum-power based associations by considering the antenna gain determined by the tilt angle in [25]. The handover rate as well as the coverage probability were analyzed by considering the practical antenna configuration [26] and also for the coordinated multi-point (CoMP) transmission [27].

However, those works considered limited scenarios and parameters of UAV networks in the design of the antenna tilt angle. For instance, in [21], [25]–[27], a simple UAV network, where ground users (GUs) do not exist, was considered in spite of using ground BSs. In [21]–[27], they considered only either the down tilt angle or the up tilt angle although both should be considered to support aerial users (AUs) together with GUs. Furthermore, only the *inclusive-service BS (IS-BS) scheme* that makes BSs serves both GUs and AUs was explored as in [22]–[24]. However, the *exclusive-service BS (ES-BS) scheme* that makes BSs serve GUs or AUs exclusively might be a better scheme for certain UAV network environments. In [22]–[24], [27], impractical parameters and modeling were also considered, such as large side lobe gain and a simplified rectangular antenna gain model, which has a constant power gain for the main lobe. Thus, insights from those works may not be applicable in practice.

Therefore, in this paper, we provide a framework to explore an appropriate BS service provisioning scheme to support both GUs and AUs with the optimum antenna tilt angle design. First, the network outage probabilities of the *ES-BS scheme* as well as the *IS-BS scheme* are derived. We then explore how the optimal antenna tilt angles of BSs that minimize the network outage probability are determined for different service provisioning schemes as well as different types of BSs. The impact of various network parameters such as the spatial densities of total BSs and interfering BSs on the performance of service provisioning schemes are also discussed. The main contributions of this paper are summarized as follows.

- We derive the network outage probability for two BS service provisioning schemes, i.e., IS-BS and ES-BS schemes. We consider the parabolic antenna gain model that has been used in 3GPP studies [28], [29]. In this model, the main lobe gain varies according to the antenna tilt angle (i.e., not constant).
- We analytically show that changing the antenna tilt angle gives conflicting impacts on the network outage probability. Specifically, as the absolute value of the tilt angle decreases, the service area with the main lobe becomes wider (i.e., positive impact), but the link distance between the serving BS and the user increases (i.e., negative impact). From these results, we show that there exists the optimal BS antenna tilt angle.
- We show the impact of various network parameters on the optimal antenna tilt angle including the UAV height, the ratio of GUs, as well as densities of the total BSs and the interfering BSs. For instance, different to [22], we show that the optimal antenna tilt angle can exist not only in the down tilt angle regime but also in the up tilt angle regime. We newly show that the optimal antenna tilt angle increases as the ratio of GUs increases.
- We also explore which service provisioning scheme can be better in terms of the network outage probability in various environments. Specifically, we *analytically* show the superiority of the ES-BS scheme to the IS-BS scheme for the high BS density regime. Furthermore, we numerically show the superiority of the IS-BS scheme for the low interfering BS density regime and that of the ES-BS scheme for the high interfering BS density regime.

The rest of this paper is organized as follows. In Section II, we represent the BS service provisioning schemes to serve

TABLE 1. Notations used throughout the paper.

Notation	Definition
$i \in \{\mathrm{G}, \mathrm{A}\}$	User type index for GUs ($i=\mathrm{G}$) and AUs ($i=\mathrm{A}$)
$l \in \{\mathrm{O}, \mathrm{G}, \mathrm{A}\}$	BS type index for IS-BS ($l = \mathrm{O}$), GBS ($l = \mathrm{G}$) and ABS ($l = \mathrm{A}$)
$v \in \{\mathrm{L}, \mathrm{N}\}$	Index for the LoS environment ($v = \mathrm{L}$) and the non-line-of-sight (NLoS) environment ($v = \mathrm{N}$)
$s \in \{\mathrm{IS}, \mathrm{ES}\}$	Index for the IS-BS scheme ($s = \mathrm{IS}$) and the ES-BS scheme ($s = \mathrm{ES}$)
$r_{k,\mathbf{x}}$	Horizontal distance between the kth user and the BS located at $\mathbf{x}$
h_B / h_k	Height of the BS and the kth user
$\Omega_{k,\mathbf{x}}$	Channel fading between the kth user and the BS
$\theta^{\mathrm{IS}}_{\mathrm{t,O}}$ / $\theta^{\mathrm{ES}}_{\mathrm{t,G}}$, $\theta^{\mathrm{ES}}_{\mathrm{t,A}}$	Antenna tilt angle of the IS-BS / Antenna tilt angles of GBS and ABS in the ES-BS scheme.
P_t	Transmission power of the BS
γ_t	Target SINR/SNR
$l_v(r_{k,\mathbf{x}})$	Path loss between the kth user and the BS
$p_\mathrm{L}(r_{k,\mathbf{x}})$ / $p_\mathrm{N}(r_{k,\mathbf{x}})$	LoS and NLoS probability for given $r_{k,\mathbf{x}}$
$G(r_{k,\mathbf{x}}, \theta_\mathrm{t})$	Antenna power gain for given $r_{k,\mathbf{x}}$ and θ_t
$r^{\mathrm{lb}}_\mathrm{G}(\theta_\mathrm{t})$ / $r^{\mathrm{lb}}_\mathrm{A}(\theta_\mathrm{t})$	Lower bound of the horizontal distance that the user is served by main lobe for GUs and AUs
$r^{\mathrm{ub}}_\mathrm{G}(\theta_\mathrm{t})$ / $r^{\mathrm{ub}}_\mathrm{A}(\theta_\mathrm{t})$	Upper bound of the horizontal distance that the user is served by main lobe for GUs and AUs
$f^{s,a}_{r^{vj}_{k,\mathbf{x}_\tau}}(r)$	PDF of the horizontal distance between the kth user and the serving BS for given scheme s and association rule a
ρ_i	Ratio of i-type users to total users
$\rho_{\mathrm{B},i}$	Ratio of BSs for i-type users to total BSs
λ_B / λ_I	Densities of total BS and total interfering BS
$\lambda^s_{\mathrm{B},i}$	BS density for i-type users in scheme s
$\lambda^{\mathrm{IS}}_{\mathrm{I,O}}$ / $\lambda^{\mathrm{ES}}_{\mathrm{I,G}}$, $\lambda^{\mathrm{ES}}_{\mathrm{I,A}}$	Density of interfering IS-BS / Densities of interfering GBS and ABS in the ES-BS scheme.
$I^{\mathrm{IS}}_\mathrm{O}$ / $I^{\mathrm{ES}}_\mathrm{G}$, $I^{\mathrm{ES}}_\mathrm{A}$	Interference from IS-BSs / Interference from GBSs and ABSs in the ES-BS scheme.
$\mathcal{P}^s_{\mathrm{no}}(\theta^s_{\mathrm{t,G}}, \theta^s_{\mathrm{t,A}})$	Network outage probability for given s

both types of users and describe the channel model and the BS antenna power gain, which is affected by the BS antenna tilt angle. We then describe the BS association rule. In Section III, we derive and analyze the network outage probability for two service provisioning schemes. In Section IV, we evaluate the network outage probability according to the various network design parameters. We then compare the communication performance of the IS-BS scheme and that of the ES-BS scheme for network parameters. Finally, conclusions are presented in V.

Notation: The notation used throughout the paper is listed in Table 1.

II. SYSTEM MODEL

In this section, we introduce the non-terrestrial network model by mainly focusing on UAV networks. Moreover, we describe the antenna power gain and the BS association rules.

A. NETWORK MODEL

We consider a NTN for UAVs, where BSs, ground users (GUs), and aerial users (AUs) (i.e., UAVs) are randomly distributed in the spatial domain. The locations of users are modeled by homogeneous Poisson point process (HPPP) $\Phi_{\mathrm{U},i}$ with density λ_i, where $i \in \{\mathrm{G}, \mathrm{A}\}$ denotes the type of user, i.e., $i = \mathrm{G}$ for GUs and $i = \mathrm{A}$ for AUs.[1] The height of the kth user is h_k, where $h_k = h_\mathrm{G}$ for $k \in \mathcal{U}_\mathrm{G}$ and $h_k = h_\mathrm{A}$ for $k \in \mathcal{U}_\mathrm{A}$. Here $\mathcal{U}_\mathrm{G}$ and $\mathcal{U}_\mathrm{A}$ are the user index sets of GUs and AUs, respectively.

In this paper, as shown in Figure 1, we consider two types of BS service provisioning schemes as follows.

- *Inclusive-service BS (IS-BS) scheme*: In this scheme, BSs serve both GUs and AUs simultaneously. Hence, the antenna tilt angle of the BS has to be designed to serve both GUs and AUs efficiently. The locations of BSs are modeled by HPPP $\Phi_{\mathrm{B,O}}$ with density λ_B. Since there is only one type of BS, the BS density for GUs, $\lambda^{\mathrm{IS}}_{\mathrm{B,G}}$, and the BS density for AUs, $\lambda^{\mathrm{IS}}_{\mathrm{B,A}}$, are the same as the total BS density (i.e., $\lambda^{\mathrm{IS}}_{\mathrm{B,G}} = \lambda^{\mathrm{IS}}_{\mathrm{B,A}} = \lambda_\mathrm{B}$). Note that this scheme is the one, generally used in prior works such as [21], [22], [24].
- *Exclusive-service BS (ES-BS) scheme*: In this scheme, BSs are divided into two groups: 1) a BS for GUs (BS for GUs (GBS)) and 2) a BS for AUs (BS for AUs (ABS)). The GBSs and ABSs exclusively serve GUs and AUs, respectively. Therefore, the antenna tilt angles of GBSs and ABSs need to be designed respectively to serve aimed users efficiently. We assume the locations of GBSs and ABSs also modeled by HPPPs, $\Phi_{\mathrm{B,G}}$ and $\Phi_{\mathrm{B,A}}$, with densities $\lambda^{\mathrm{ES}}_{\mathrm{B,G}} = \rho_{\mathrm{B,G}}\lambda_\mathrm{B}$ and $\lambda^{\mathrm{ES}}_{\mathrm{B,A}} = (1-\rho_{\mathrm{B,G}})\lambda_\mathrm{B}$, respectively, where $\rho_{\mathrm{B,G}}$ is the portion of GBSs among all BSs.

Regardless of BS types, for all BSs, the antenna height is h_B and the transmission power is P_t.

B. CHANNEL MODEL

In UAV communications, both LoS and NLoS environments can be considered for the links between a BS and a GU as well as between a BS and an AU. The probability of forming LoS link between the BS at $\mathbf{x} = (x_\mathrm{B}, y_\mathrm{B}, h_\mathrm{B})$ and the kth user at (x_k, y_k, h_k) is given by [32][2]

$$p_\mathrm{L}(r_{k,\mathbf{x}}) = \left\{1 - \frac{\sqrt{2\pi}\xi}{|h_k - h_\mathrm{B}|}\left|Q\left(\frac{h_k}{\xi}\right) - Q\left(\frac{h_\mathrm{B}}{\xi}\right)\right|\right\}^{r_{k,\mathbf{x}}\sqrt{\mu\nu}}, \tag{1}$$

[1]Note that we can also assume AUs are distributed according to Matérn Hardcore Point Processes (MHCPP) with density λ_A that considers the minimum safety horizontal distance, $d_{\min}$, between any two AUs like the ones in [30], [31]. However, the performance analysis and the results of this work will be the same as only the density of AUs affects the performance, not the distribution as the downlink is considered.

[2]The LoS probability is also defined differently in [9]. However, it is determined by the elevation angle between the transmitter and the receiver, not by the link distance.

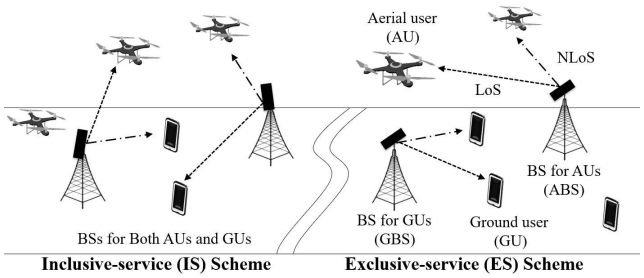

FIGURE 1. Examples of NTN for UAVs with randomly distributed BSs, GUs, and AUs.

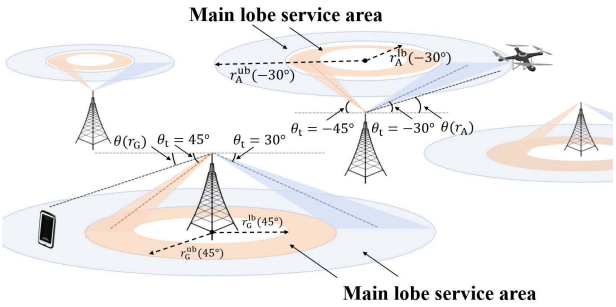

FIGURE 2. Examples of antenna radiation patterns for different antenna tilt angles.

where $Q(x) = \int_x^\infty \frac{1}{\sqrt{2\pi}} \exp(-\frac{t^2}{2})\, dt$ is the Q-function and the horizontal distance between the BS and the kth user is given by $r_{k,\mathbf{x}} = \sqrt{(x_k - x_\mathrm{B})^2 + (y_k - y_\mathrm{B})^2}$. Here, μ is the ratio of land area covered by buildings to total land area, ν is the mean number of buildings per unit area, and ξ is a variable determining the building height distribution. Since the NLoS environment is a complementary event of the LoS environment, the NLoS probability between the BS and the kth user is given by $p_\mathrm{N}(r_{k,\mathbf{x}}) = 1 - p_\mathrm{L}(r_{k,\mathbf{x}})$.

Based on the LoS probability, we consider different path loss exponents and channel fading models for LoS and NLoS links. The path loss exponent for LoS and NLoS links are denoted by α_L and α_N, respectively. The channel fading is modeled by Nakagami-m fading, so the distribution of the channel gain is given by

$$f_{\Omega_v}(x) = \frac{m_v^{m_v}}{\Gamma(m_v)} x^{m_v - 1} \exp\left(-m_v x\right), \quad x > 0, \tag{2}$$

where $\Gamma(x) = \int_0^\infty t^{x-1} e^{-t} dt$ and $v \in \{\mathrm{L}, \mathrm{N}\}$ is the channel environment, i.e., $v = \mathrm{L}$ for LoS links and $v = \mathrm{N}$ for NLoS links. In addition, we assume that $m_\mathrm{L} > 1$, and $m_\mathrm{N} = 1$, which means Rayleigh fading, i.e., $\Omega_\mathrm{N} \sim \exp(1)$. From (2), we denote the channel fading between the kth user and the BS as

$$\Omega_{k,\mathbf{x}} = \begin{cases} \Omega_\mathrm{L}, & \text{with probability } p_\mathrm{L}(r_{k,\mathbf{x}}) \\ \Omega_\mathrm{N}, & \text{otherwise.} \end{cases} \tag{3}$$

C. VERTICAL ANTENNA GAIN

The antenna power gain of the BS is determined by two types of power gains: horizontal and vertical directional antenna gains. We consider an omnidirectional antenna in the horizontal direction, so the horizontal directional antenna gain remains constant regardless of the direction of the antenna. Therefore, we assume the horizontal directional antenna gain is equal to a unit gain [33]. In this paper, we focus on the design of the vertical antenna tilt angle for AUs as well as GUs, and we consider the directional antenna in the vertical direction. As shown in Fig. 2, the vertical directional antenna gain is determined by the vertical antenna tilt angle, $-90° < \theta_\mathrm{t} < 90°$, which is the angle tilted upward or downward relative to the horizontal plane.[3] Here, we define that the BS antenna tilt angle is a negative value when the BS antenna tilt angle is up-tilted, i.e., tilting upwards with respect to the horizontal plane of the BS antenna. On the other hand, the BS antenna tilt angle is defined as a positive value when the BS antenna tilt angle is down-tilted, i.e., tilting downwards with respect to the horizontal plane of the BS antenna. Based on the 3GPP specification [28], the BS antenna power gain $G(r_{k,\mathbf{x}}, \theta_\mathrm{t})$ can be represented as

$$G\left(r_{k,\mathbf{x}}, \theta_\mathrm{t}\right) = 10^{-\min\left(12\left(\frac{\theta(r_{k,\mathbf{x}}) + \theta_\mathrm{t}}{\theta_{3\mathrm{dB}}}\right)^2, \eta\right)/10}, \tag{4}$$

where $\theta_{3\mathrm{dB}} = 10°$ is the 3dB beamwidth and η is the minimum power leaking to the side lobe besides the main lobe, which is commonly 20dB. In (4), $\theta\left(r_{k,\mathbf{x}}\right)$ is the elevation angle between the BS antenna and the kth user, which is given by

$$\theta\left(r_{k,\mathbf{x}}\right) = \frac{180}{\pi} \arctan\left(\frac{h_k - h_\mathrm{B}}{r_{k,\mathbf{x}}}\right), \tag{5}$$

where $h_k - h_\mathrm{B}$ is the height difference between the BS and the kth user. In this work, without loss of generality, we assume that the height of AUs is higher than that of BSs (i.e., $h_\mathrm{A} - h_\mathrm{B} > 0$), while the height of GUs is lower than that of BSs (i.e., $h_\mathrm{G} - h_\mathrm{B} < 0$). From (4), for given θ_t, the user can be served with the main lobe when $12\left(\frac{\theta(r_{k,\mathbf{x}}) + \theta_\mathrm{t}}{\theta_{3\mathrm{dB}}}\right)^2 \geq \eta$. Here, we define the boundary of horizontal distance between a BS and the kth user that the user is served by the main lobe as $r_k^{\mathrm{lb}}(\theta_\mathrm{t}) \leq r_{k,\mathbf{x}} \leq r_k^{\mathrm{ub}}(\theta_\mathrm{t})$, where $r_k^{\mathrm{lb}}(\theta_\mathrm{t})$ and $r_k^{\mathrm{ub}}(\theta_\mathrm{t})$ are the lower and upper boundaries. Since all GUs and all AUs have the same height, h_G and h_A, respectively, the boundaries are determined by the user types not user's specific location, i.e. $r_k^{\mathrm{ub}}(\theta_\mathrm{t}) = r_i^{\mathrm{ub}}(\theta_\mathrm{t})$ and $r_k^{\mathrm{lb}}(\theta_\mathrm{t}) = r_i^{\mathrm{lb}}(\theta_\mathrm{t})$ for $k \in \mathcal{U}_i$, and given

[3] Note that there are two types of tilting methods [34]: mechanical tilting and electrical tilting. The mechanical tilting rotates the antenna of the BS physically. On the other hand, the electrical tilting applies an overall phase shift to all antenna elements in the array. In this paper, we consider the electrical tilting method to analyze the communication performance mathematically.

as follows

$$r_{\mathrm{G}}^{\mathrm{lb}}(\theta_{\mathrm{t}}) = \begin{cases} \dfrac{h_{\mathrm{G}} - h_{\mathrm{B}}}{\tan\left\{\frac{\pi}{180}(-\theta_{\mathrm{t}} - \theta_{\mathrm{th}})\right\}}, & \theta_{\mathrm{t}} > -\theta_{\mathrm{th}} \\ \infty, & \text{otherwise}, \end{cases} \tag{6}$$

$$r_{\mathrm{G}}^{\mathrm{ub}}(\theta_{\mathrm{t}}) = \begin{cases} \dfrac{h_{\mathrm{G}} - h_{\mathrm{B}}}{\tan\left\{\frac{\pi}{180}(-\theta_{\mathrm{t}} + \theta_{\mathrm{th}})\right\}}, & \theta_{\mathrm{t}} > \theta_{\mathrm{th}} \\ \infty, & \text{otherwise}, \end{cases} \tag{7}$$

$$r_{\mathrm{A}}^{\mathrm{lb}}(\theta_{\mathrm{t}}) = \begin{cases} \dfrac{h_{\mathrm{A}} - h_{\mathrm{B}}}{\tan\left\{\frac{\pi}{180}(-\theta_{\mathrm{t}} + \theta_{\mathrm{th}})\right\}}, & \theta_{\mathrm{t}} < \theta_{\mathrm{th}} \\ \infty, & \text{otherwise} \end{cases} \tag{8}$$

$$r_{\mathrm{A}}^{\mathrm{ub}}(\theta_{\mathrm{t}}) = \begin{cases} \dfrac{h_{\mathrm{A}} - h_{\mathrm{B}}}{\tan\left\{\frac{\pi}{180}(-\theta_{\mathrm{t}} - \theta_{\mathrm{th}})\right\}}, & \theta_{\mathrm{t}} < -\theta_{\mathrm{th}} \\ \infty, & \text{otherwise}, \end{cases} \tag{9}$$

where $\theta_{\mathrm{th}} = \theta_{3\mathrm{dB}}\sqrt{\eta/12}$. In (6)-(9), the boundaries $r_i^{\mathrm{ub}}(\theta_{\mathrm{t}})$ and $r_i^{\mathrm{lb}}(\theta_{\mathrm{t}})$ are defined to be positive when θ_{t} satisfies each conditions. For the convenience of analysis, we rewrite $G\left(r_{k,\mathbf{x}}, \theta_{\mathrm{t}}\right)$ in (4) according to the boundaries in (6)-(9) as

$$G\left(r_{k,\mathbf{x}}, \theta_{\mathrm{t}}\right) = \begin{cases} G_1(r_{k,\mathbf{x}}, \theta_{\mathrm{t}}), & b_{k,1}(\theta_{\mathrm{t}}) < r_{k,\mathbf{x}} < b_{k,2}(\theta_{\mathrm{t}}) \\ G_2(r_{k,\mathbf{x}}, \theta_{\mathrm{t}}), & b_{k,2}(\theta_{\mathrm{t}}) \le r_{k,\mathbf{x}} \le b_{k,3}(\theta_{\mathrm{t}}) \\ G_3(r_{k,\mathbf{x}}, \theta_{\mathrm{t}}), & b_{k,3}(\theta_{\mathrm{t}}) < r_{k,\mathbf{x}} < b_{k,4}(\theta_{\mathrm{t}}), \end{cases} \tag{10}$$

where $b_{k,1}(\theta_{\mathrm{t}}) = 0, b_{k,2}(\theta_{\mathrm{t}}) = r_k^{\mathrm{lb}}(\theta_{\mathrm{t}}), b_{k,3}(\theta_{\mathrm{t}}) = r_k^{\mathrm{ub}}(\theta_{\mathrm{t}})$, and $b_{k,4}(\theta_{\mathrm{t}}) = \infty$. In (10), $G_1(r_{k,\mathbf{x}}, \theta_{\mathrm{t}}) = G_3(r_{k,\mathbf{x}}, \theta_{\mathrm{t}}) = 10^{-\eta/10}$ is the antenna side lobe gain and $G_2(r_{k,\mathbf{x}}, \theta_{\mathrm{t}})$ is the antenna main lobe gain, which is given by

$$G_2(r_{k,\mathbf{x}}, \theta_{\mathrm{t}}) = 10^{-1.2\left\{\frac{\theta(r_{k,\mathbf{x}}) + \theta_{\mathrm{t}}}{\theta_{3\mathrm{dB}}}\right\}^2}. \tag{11}$$

From (11), we can see that $G_2(r_{k,\mathbf{x}}, \theta_{\mathrm{t}})$ is an increasing function of θ_{t} for $-\theta_{\mathrm{th}} < \theta_{\mathrm{t}} \le -\theta\left(r_{k,\mathbf{x}}\right)$, and $G_2(r_{k,\mathbf{x}}, \theta_{\mathrm{t}})$ is a decreasing function of θ_{t} for $-\theta\left(r_{k,\mathbf{x}}\right) \le \theta_{\mathrm{t}} < \theta_{\mathrm{th}}$. This is because as the antenna tilt angle θ_{t} approaches the elevation angle between the BS and the user, the effect of the main lobe becomes dominant and it is maximized when the antenna tilt angle is equal to the elevation angle (i.e., $\theta_{\mathrm{t}} = -\theta\left(r_{k,\mathbf{x}}\right)$).

D. BS ASSOCIATION RULE

In conventional networks, the BS association is determined by the mean channel fading gain and the distance-dependent path loss, considering the LoS probability [35]. However, in more realistic UAV networks, the antenna gain $G\left(r_{k,\mathbf{x}}, \theta_{\mathrm{t}}\right)$ affected by the horizontal distance between the serving BS and the kth user should also be considered in the BS association.

To analyze BS association rules, we first denote BSs which belong to $\Phi_{\mathrm{B},l}, l \in \{\mathrm{O},\mathrm{G},\mathrm{A}\}$, forming LoS and NLoS links as $\Phi_{\mathrm{B},l}^{\mathrm{L}}$ and $\Phi_{\mathrm{B},l}^{\mathrm{N}}$, respectively. We then divide each of $\Phi_{\mathrm{B},l}^{\mathrm{L}}$ and $\Phi_{\mathrm{B},l}^{\mathrm{N}}$ into three groups according to the BS antenna power gain $G\left(r_{k,\mathbf{x}}, \theta_{\mathrm{t}}\right)$ in (10) as

$$\Phi_{\mathrm{B},l}^{vj} = \begin{cases} \Phi_{\mathrm{B},l}^{v1}, & b_{k,1}(\theta_{\mathrm{t}}) < r_{k,\mathbf{x}} < b_{k,2}(\theta_{\mathrm{t}}) \\ \Phi_{\mathrm{B},l}^{v2}, & b_{k,2}(\theta_{\mathrm{t}}) \le r_{k,\mathbf{x}} \le b_{k,3}(\theta_{\mathrm{t}}) \\ \Phi_{\mathrm{B},l}^{v3}, & b_{k,3}(\theta_{\mathrm{t}}) < r_{k,\mathbf{x}} < b_{k,4}(\theta_{\mathrm{t}}), \end{cases} \quad v \in \{\mathrm{L},\mathrm{N}\}, \tag{12}$$

where $j \in \mathcal{J}$ is the index of BS groups which is determined by $r_{k,\mathbf{x}}$, and $\mathcal{J} = \{1, 2, 3\}$. Note that from (10) and (12), we know that BSs in $\Phi_{\mathrm{B},l}^{v1}$ or $\Phi_{\mathrm{B},l}^{v3}$ transmit with the antenna side lobe gain, and BSs in $\Phi_{\mathrm{B},l}^{v2}$ transmit with the antenna main lobe gain. First of all, we examine the distribution of the distance between the user and the BS in $\Phi_{\mathrm{B},l}^{vj}$. The horizontal distance to the nearest BS among the BSs in $\Phi_{\mathrm{B},l}^{vj}$ is denoted by X_k^{vj}. Here, depending on the LoS probability, the density function of $\Phi_{\mathrm{B},l}^{vj}$ is given by $2\pi\lambda_{\mathrm{B},k}^s t p_v(t)$. Therefore, for BSs in $\Phi_{\mathrm{B},l}^{vj}$, the complementary cumulative distribution function (CCDF) of X_k^{vj} can be obtained as

$$\begin{aligned} \bar{F}_{X_k^{vj}}^s(x) &= \mathbb{P}\left[X_k^{vj} \ge x\right] \\ &\overset{(a)}{=} \exp\left\{-2\pi\lambda_{\mathrm{B},k}^s \int_{b_{k,j}(\theta_{\mathrm{t}})}^{u_{k,j}(x,\theta_{\mathrm{t}})} t p_v(t) dt\right\}, \end{aligned} \tag{13}$$

where (a) is from the void probability [36] and $u_{k,j}(x, \theta_{\mathrm{t}})$ is given as $u_{k,1}(x, \theta_{\mathrm{t}}) = \min(x, b_{k,j+1}(\theta_{\mathrm{t}}))$ if $j = 1$, $u_{k,j}(x, \theta_{\mathrm{t}}) = \max(x, b_{k,j}(\theta_{\mathrm{t}}))$, otherwise. $\lambda_{\mathrm{B},k}^s$ is the density of BSs that can serve the kth user, i.e., $\lambda_{\mathrm{B},k}^s = \lambda_{\mathrm{B},i}^s$ when $k \in \mathcal{U}_i$. Here, $s \in \{\mathrm{IS},\mathrm{ES}\}$ is the index of the BS service provisioning scheme. By differentiating (13), we can obtain the probability distribution function (PDF) of X_k^{vj} as

$$f_{X_k^{vj}}^s(x) = 2\pi\lambda_{\mathrm{B},k}^s x p_v(x) \exp\left\{-2\pi\lambda_{\mathrm{B},k}^s \int_{b_{k,j}(\theta_{\mathrm{t}})}^{x} t p_v(t) dt\right\}, \tag{14}$$

where $f_{X_k^{vj}}^s(x) = 0$ if $x \le b_{k,j}(\theta_{\mathrm{t}})$.

We denote $a \in \{\mathrm{na}, \mathrm{sa}\}$ as the index of the BS association criterion. Here, $a = \mathrm{na}$ and $a = \mathrm{sa}$ indicate the nearest BS association rule and the strongest BS association rule, respectively.

1) NEAREST BS ASSOCIATION RULE

In the nearest BS association rule ($a = \mathrm{na}$), the horizontal distance between the kth user and the serving BS is smallest. Therefore, the probability that the serving BS exists in $\Phi_{\mathrm{B},l}^{vj}$, and the horizontal distance between the serving BS and the kth user is smaller than r is given by

$$\begin{aligned} &\mathbb{P}\left[X_k^{vj} \le r, \mathbf{x}_\tau \in \Phi_{\mathrm{B},l}^{vj} \mid a = \mathrm{na}\right] \\ &\overset{(a)}{=} \int_{b_{k,j}(\theta_{\mathrm{t}})}^{r} f_{X_k^{vj}}^s(x) \prod_{\substack{j_o \in \mathcal{J}, v_o \in \{\mathrm{L},\mathrm{N}\}, \\ (j_o, v_o) \ne (j, v)}} \mathbb{P}\left[x \le X_k^{v_o j_o}\right] dx. \\ &= \int_{b_{k,j}(\theta_{\mathrm{t}})}^{r} f_{X_k^{vj}}^s(x) \prod_{\substack{j_o \in \mathcal{J}, v_o \in \{\mathrm{L},\mathrm{N}\}, \\ (j_o, v_o) \ne (j, v)}} \bar{F}_{X_k^{v_o j_o}}^s(x) dx, \end{aligned} \tag{15}$$

where $\mathbf{x}_\tau$ denotes the location of the serving BS and (a) is from the fact that for given j and v, the horizontal distance between the serving BS and the user is shorter than all other candidates.

2) STRONGEST BS ASSOCIATION RULE

In the strongest BS association rule ($a = \mathrm{s}$), the main link has the strongest average received power. The probability that the serving BS exists in $\Phi_{\mathrm{B},l}^{vj}$ and the horizontal distance between the serving BS and the kth user is smaller than r is given in (16), as shown at the bottom of the page. In (16), (a) is from the fact that for given j and v, the average power of the serving BS should be greater than all other candidates.

From (15) and (16), given $a \in \{\mathrm{na}, \mathrm{sa}\}$, we can obtain the association probability $\mathcal{A}_{vj}^{a}$ as

$$\mathcal{A}_{vj}^{a} = \mathbb{P}\left[X_k^{vj} \le b_{k,j+1}(\theta_\mathrm{t}), \mathbf{x}_\tau \in \Phi_{\mathrm{B},l}^{vj} \mid a\right]. \tag{17}$$

Therefore, when the kth user is associated with a BS in j-group under the channel environment v, the cumulative distribution function (CDF) of the horizontal distance between the BS and the user, $r_{k,\mathbf{x}_\tau}^{vj}$, is given by

$$F_{r_{k,\mathbf{x}_\tau}^{vj}}^{s,a}(r) = \mathbb{P}\left[X_k^{vj} \le r, \mathbf{x}_\tau \in \Phi_{\mathrm{B},l}^{vj} \mid a\right] / \mathcal{A}_{vj}^{a}. \tag{18}$$

Note that the distribution of the horizontal distance between the serving BS and the kth user, $r_{k,\mathbf{x}_\tau}^{vj}$, is the same for all i-type users, so we use i index only without using k index in the followings, i.e., $r_{k,\mathbf{x}_\tau}^{vj} = r_i^{vj}$ for $k \in \mathcal{U}_i$. By differentiating (18), we can obtain the PDF of r_i^{vj}, which is given by

$$f_{r_i^{vj}}^{s,a}(r) = \begin{cases} \dfrac{2\pi\lambda_{\mathrm{B},i}^{s} x p_v(x)}{\mathcal{A}_{vj}^{\mathrm{na}}} \\ \quad \times \exp\left\{-2\pi\lambda_{\mathrm{B},i}^{s}\displaystyle\int_{b_{k,j}(\theta_\mathrm{t})}^{x} t p_v(t)dt\right\}, & a = \mathrm{na} \\ \dfrac{\partial}{\partial r} F_{r_{k,\mathbf{x}_\tau}^{vj}}^{s,\mathrm{sa}}(r), & a = \mathrm{sa}. \end{cases} \tag{19}$$

Note that $f_{r_i^{vj}}^{s,\mathrm{sa}}(r)$ cannot be presented due to the complicated form of (16). However, in Section IV, we show that the performance of the strongest association and that of the nearest association have similar trends. This means we can use the analysis of the nearest association to design the case of the strongest association as well.

III. OUTAGE PROBABILITY ANALYSIS

In this section, for both IS-BS and ES-BS schemes, we derive the network outage probability in the presence of GUs and AUs. We then analyze the impact of the antenna tilt angle on network outage probability.

We assume that the available frequency resource is divided into N sub-bands, and the interfering BSs are the ones that use the same sub-band. Hence, in the IS-BS scheme, the distribution of the interfering BSs is modeled as a HPPP $\Phi_{\mathrm{I,O}}$ with density $\lambda_{\mathrm{I,O}}^{\mathrm{IS}} = \lambda_\mathrm{B}/N$ such as in [37]. In the ES-BS scheme, the interference from GBSs and ABSs needs to be defined differently as they use different tilt angles. The distributions of interfering GBSs and ABSs are also modeled as HPPPs, $\Phi_{\mathrm{I,G}}$ and $\Phi_{\mathrm{I,A}}$, with densities $\lambda_{\mathrm{I,G}}^{\mathrm{ES}} = \lambda_{\mathrm{B,G}}^{\mathrm{ES}}/N$ and $\lambda_{\mathrm{I,A}}^{\mathrm{ES}} = \lambda_{\mathrm{B,A}}^{\mathrm{ES}}/N$, respectively.

For the case that the serving BS communicates with the kth user, the SINR at the user can be given by

$$\gamma_v^s(r_{k,\mathbf{x}_\tau}, \theta_\mathrm{t}) = \frac{P_\mathrm{t}\Omega_{k,v} l_v\left(r_{k,\mathbf{x}_\tau}\right) G\left(r_{k,\mathbf{x}_\tau}, \theta_\mathrm{t}\right)}{I^s + \sigma^2}, \tag{20}$$

where $l_v\left(r_{k,\mathbf{x}_\tau}\right) = \left(r_{k,\mathbf{x}}^2 + (h_k - h_\mathrm{B})^2\right)^{-\frac{\alpha_v}{2}}$, $v \in \{\mathrm{L}, \mathrm{N}\}$, is the distance-dependent path loss between the kth user and the serving BS at $\mathbf{x}_\tau$ for LoS and NLoS links, and σ^2 is the noise power. In (20), $I^{\mathrm{IS}} = I_\mathrm{O}^{\mathrm{IS}}$ and $I^{\mathrm{ES}} = I_\mathrm{G}^{\mathrm{ES}} + I_\mathrm{A}^{\mathrm{IS}}$, where I_l^s is given by

$$I_l^s = \sum_{\mathbf{x}\in\Phi_{\mathrm{I},l}\setminus\{\mathbf{x}_\tau\}} P_\mathrm{t}\Omega_{k,\mathbf{x}} l_v\left(r_{k,\mathbf{x}}\right) G(r_{k,\mathbf{x}}, \theta_\mathrm{t}). \tag{21}$$

Using the SINR in (20), when the user associates to a j-group BS with the distance $r_{k,\mathbf{x}_\tau}$ and the tilt angle θ_t under the channel environment v, the outage probability is given by

$$\mathcal{P}_{\mathrm{o},j}^{v}(r_{k,\mathbf{x}_\tau}, \theta_\mathrm{t}) = \mathbb{P}\left[\gamma_v^s(r_{k,\mathbf{x}_\tau}, \theta_\mathrm{t}) < \gamma_\mathrm{t}\right], \tag{22}$$

where $\gamma_\mathrm{t} = 2^{\frac{R_\mathrm{o}}{W}} - 1$ is the target SINR. Here, R_o is the target data rate and W is the bandwidth allocated to each user [38].

For readability, instead of using the notation θ_t, when scheme s is used, we denote antenna tilt angles of the GBS and the ABS as $\theta_{\mathrm{t,G}}^s$ and $\theta_{\mathrm{t,A}}^s$, respectively. Note that in the IS-BS scheme, since all BSs serve both GUs and AUs, we have a single antenna tilt angle $\theta_{\mathrm{t,O}}^{\mathrm{IS}}$, i.e., $\theta_{\mathrm{t,G}}^{\mathrm{IS}} = \theta_{\mathrm{t,A}}^{\mathrm{IS}} = \theta_{\mathrm{t,O}}^{\mathrm{IS}}$. Using similar steps in [22], [23], the network outage probability can be obtained as the following theorem.

Theorem 1: For IS-BS ($s = \mathrm{IS}$) and ES-BS ($s = \mathrm{ES}$) schemes, the network outage probability can be presented as

$$\mathbb{P}\left[X_k^{vj} \le r, \mathbf{x}_\tau \in \Phi_{\mathrm{B},l}^{vj} \mid a = \mathrm{sa}\right] \overset{(a)}{=} \int_{b_{k,j}(\theta_\mathrm{t})}^{r} f_{X_k^{vj}}^{s}(x) \prod_{\substack{j_o\in\mathcal{J}, v_o\in\{\mathrm{L},\mathrm{N}\},\\ (j_o,v_o)\neq(j,v)}} \mathbb{P}\left[G_j(x,\theta_\mathrm{t})\left(x^2+h_k^2\right)^{-\frac{\alpha_v}{2}} \ge G_{j_o}\left(X_k^{v_o j_o}, \theta_\mathrm{t}\right)\left((X_k^{v_o j_o})^2 + h_k^2\right)^{-\frac{\alpha_{v_o}}{2}}\right] dx \tag{16}$$

a function of BS antenna tilt angles $\left(\theta^s_{\mathrm{t,G}}, \theta^s_{\mathrm{t,A}}\right)$ as

$$\mathcal{P}^s_{\mathrm{no}}(\theta^s_{\mathrm{t,G}}, \theta^s_{\mathrm{t,A}}) = \rho_{\mathrm{G}}\mathcal{P}^s_{\mathrm{no,G}}(\theta^s_{\mathrm{t,G}}) + \rho_{\mathrm{A}}\mathcal{P}^s_{\mathrm{no,A}}(\theta^s_{\mathrm{t,A}}),\ s \in \{\mathrm{IS}, \mathrm{ES}\}, \quad (23)$$

where $\rho_i = \lambda_i/(\lambda_{\mathrm{G}} + \lambda_{\mathrm{A}})$ is the ratio of the density of i-type users to that of total users, $i \in \{\mathrm{G,A}\}$, and the outage probability of i-type users $\mathcal{P}^s_{\mathrm{no},i}(\theta^s_{\mathrm{t},i})$ is given by

$$\mathcal{P}^s_{\mathrm{no},i}(\theta^s_{\mathrm{t},i}) = \sum_{\substack{j\in\mathcal{J},\\ v\in\{\mathrm{L,N}\}}} \left(\int_{b_{i,j}(\theta^s_{\mathrm{t},i})}^{b_{i,j+1}(\theta^s_{\mathrm{t},i})} \mathcal{A}^a_{vj}\mathcal{P}^v_{\mathrm{o},j}(r, \theta^s_{\mathrm{t},i}) f^{s,a}_{r^{vj}_i}(r) dr \right), \quad (24)$$

where $f^{s,a}_{r^{vj}_i}(r)$ is given in (19) and $\mathcal{P}^v_{\mathrm{o},j}(r, \theta^s_{\mathrm{t},i})$ is given by

$$\mathcal{P}^v_{\mathrm{o},j}(r, \theta^s_{\mathrm{t},i}) = 1 - \sum_{n=0}^{m_v-1} \left[\frac{(-z)^n}{n!} \frac{d^n}{dz^n} \exp\left(-z\sigma^2\right) \mathcal{L}_{I^s}(z) \right]_{z=\frac{m_v\gamma_t}{P_t l_v(r) G_j(r,\theta^s_{\mathrm{t},i})}}, \quad (25)$$

where $\mathcal{L}_{I^{\mathrm{IS}}}(z) = \mathcal{L}_{I^{\mathrm{IS}}_{\mathrm{O}}}(z)$ and $\mathcal{L}_{I^{\mathrm{ES}}}(z) = \mathcal{L}_{I^{\mathrm{ES}}_{\mathrm{G}}}(z)\mathcal{L}_{I^{\mathrm{ES}}_{\mathrm{A}}}(z)$, and $\mathcal{L}_{I^s_l}(z)$ is the Laplace transform of the interference from l-type BSs, $l \in \{\mathrm{O,G,A}\}$, for the BS service provisioning scheme s, given in (26), as shown at the bottom of the page. In (26), $c_{i,j}(r, \theta^s_{\mathrm{t},l}) = \min\left[b_{i,j+1}(\theta^s_{\mathrm{t},l}), \max(r, b_{i,j}(\theta^s_{\mathrm{t},l}))\right]$.

Proof: See Appendix. ∎

From Theorem 1, we can obtain the network outage probabilities for two types of service provisioning schemes, which consider different channel fadings for LoS and NLoS environments. Here, we can see that the network outage probability is affected by the main lobe service area that the BS can serve with the strong main lobe gain, i.e., the area with distance $r^{\mathrm{lb}}_i(\theta^s_{\mathrm{t},i})(= b_{k,2})$ to $r^{\mathrm{ub}}_i(\theta^s_{\mathrm{t},i})(= b_{k,3})$ from the BS (see Fig. 2). Note that different to [22] and [23], which considers GUs and AUs only with the constant main lobe gain, the network outage probability is derived considering both GUs and AUs with more realistic main lobe antenna gain that follows the parabolic function as in (11). Therefore, the network outage probability in (23) shows different performance to the one in [22] and [23], which is verified in Fig. 5 of Section IV.

The main lobe service area is determined by the antenna tilt angle, and the effect of the antenna tilt angle on $\left|r^{\mathrm{ub}}_i(\theta^s_{\mathrm{t},i}) - r^{\mathrm{lb}}_i(\theta^s_{\mathrm{t},i})\right|$ is presented in the following corollary.

Corollary 1: For $\theta_{\mathrm{th}} < \theta^s_{\mathrm{t,G}} < \frac{\pi}{2}$ and $-\frac{\pi}{2} < \theta^s_{\mathrm{t,A}} < -\theta_{\mathrm{th}}$, $\left|r^{\mathrm{ub}}_{\mathrm{G}}(\theta^s_{\mathrm{t,G}}) - r^{\mathrm{lb}}_{\mathrm{G}}(\theta^s_{\mathrm{t,G}})\right|$ and $\left|r^{\mathrm{ub}}_{\mathrm{A}}(\theta^s_{\mathrm{t,A}}) - r^{\mathrm{lb}}_{\mathrm{A}}(\theta^s_{\mathrm{t,A}})\right|$ increase, as $\theta^s_{\mathrm{t,G}}$ and $\theta^s_{\mathrm{t,A}}$ approach θ_{th} and $-\theta_{\mathrm{th}}$, respectively.

Proof: From (6) and (7), we obtain the first derivative of $\left|r^{\mathrm{ub}}_{\mathrm{G}}(\theta^s_{\mathrm{t,G}}) - r^{\mathrm{lb}}_{\mathrm{G}}(\theta^s_{\mathrm{t,G}})\right|$ with respect to $\theta^s_{\mathrm{t,G}}$ as

$$\frac{\partial}{\partial\theta^s_{\mathrm{t,G}}}\left\{r^{\mathrm{ub}}_{\mathrm{G}}(\theta^s_{\mathrm{t,G}}) - r^{\mathrm{lb}}_{\mathrm{G}}(\theta^s_{\mathrm{t,G}})\right\} = \psi(\theta^s_{\mathrm{t,G}})(h_{\mathrm{B}} - h_{\mathrm{G}}) < 0, \quad (27)$$

for $\theta_{\mathrm{th}} < \theta^s_{\mathrm{t,G}} < \frac{\pi}{2}$, where $\psi(\theta) = \csc^2(\theta + \theta_{\mathrm{th}}) - \csc^2(\theta - \theta_{\mathrm{th}})$. In (27), the inequality is obtained since $\psi(\theta^s_{\mathrm{t,G}}) < 0$ and $h_{\mathrm{B}} - h_{\mathrm{G}} > 0$. From (8) and (9), the first derivative of $\left|r^{\mathrm{ub}}_{\mathrm{A}}(\theta^s_{\mathrm{t,A}}) - r^{\mathrm{lb}}_{\mathrm{A}}(\theta^s_{\mathrm{t,A}})\right|$ with respect to $\theta^s_{\mathrm{t,A}}$ is given by

$$\frac{\partial}{\partial\theta^s_{\mathrm{t,A}}}\left\{r^{\mathrm{ub}}_{\mathrm{A}}(\theta^s_{\mathrm{t,A}}) - r^{\mathrm{lb}}_{\mathrm{A}}(\theta^s_{\mathrm{t,A}})\right\} = \psi(\theta^s_{\mathrm{t,A}})(h_{\mathrm{A}} - h_{\mathrm{B}}) > 0, \quad (28)$$

for $-\frac{\pi}{2} < \theta^s_{\mathrm{t,A}} < -\theta_{\mathrm{th}}$. In (28), the inequality is obtained since $\psi(\theta^s_{\mathrm{t,A}}) > 0$ and $h_{\mathrm{A}} - h_{\mathrm{B}} > 0$. Therefore, we can see that $\left|r^{\mathrm{ub}}_{\mathrm{G}}(\theta^s_{\mathrm{t,G}}) - r^{\mathrm{lb}}_{\mathrm{G}}(\theta^s_{\mathrm{t,G}})\right|$ and $\left|r^{\mathrm{ub}}_{\mathrm{A}}(\theta^s_{\mathrm{t,A}}) - r^{\mathrm{lb}}_{\mathrm{A}}(\theta^s_{\mathrm{t,A}})\right|$ are monotonically decreasing function and increasing function of $\theta^s_{\mathrm{t,G}}$ and $\theta^s_{\mathrm{t,A}}$, respectively. ∎

Remark 1: From (6)-(9) and Corollary 1, we can see that $\left|r^{\mathrm{ub}}_i(\theta^s_{\mathrm{t},i}) - r^{\mathrm{lb}}_i(\theta^s_{\mathrm{t},i})\right|$, $r^{\mathrm{lb}}_i(\theta^s_{\mathrm{t},i})$, and $r^{\mathrm{ub}}_i(\theta^s_{\mathrm{t},i})$ increases, as $\theta^s_{\mathrm{t,G}}$ or $\theta^s_{\mathrm{t,A}}$ approaches θ_{th} or $-\theta_{\mathrm{th}}$, respectively. This means the main lobe service area becomes wider as $\theta^s_{\mathrm{t,G}}$ or $\theta^s_{\mathrm{t,A}}$ approaches θ_{th} or $-\theta_{\mathrm{th}}$, respectively, as also shown in Fig. 2. However, as both $r^{\mathrm{lb}}_i(\theta^s_{\mathrm{t},i})$ and $r^{\mathrm{ub}}_i(\theta^s_{\mathrm{t},i})$ increase, the link distance between the serving BS and the user, located in the main lobe service area, becomes larger, as shown in Fig. 2. Hence, the change of the antenna tilt angle gives conflicting impacts on the network outage probability, so we need to carefully determine the antenna tilt angle to improve the network performance.

Let the optimal values of the BS antenna tilt angle for the IS-BS and ES-BS schemes that minimize $\mathcal{P}^{\mathrm{IS}}_{\mathrm{no}}\left(\theta_{\mathrm{t,0}}\right)$ and $\mathcal{P}^{\mathrm{ES}}_{\mathrm{no}}\left(\theta^{\mathrm{ES}}_{\mathrm{t,G}}, \theta^{\mathrm{ES}}_{\mathrm{t,A}}\right)$ be $\theta^*_{\mathrm{t,O}}$ and $\theta^*_{\mathrm{t},i}$, $i \in \{\mathrm{G,A}\}$, respectively. In the following corollary, we compare the network outage probabilities of the IS-BS and ES-BS schemes, i.e., $\mathcal{P}^{\mathrm{IS}}_{\mathrm{no}}\left(\theta^*_{\mathrm{t,O}}\right)$ and $\mathcal{P}^{\mathrm{ES}}_{\mathrm{no}}\left(\theta^*_{\mathrm{t,G}}, \theta^*_{\mathrm{t,A}}\right)$, for given the optimal tilt angle.

$$\mathcal{L}_{I^s_l}(z) = \exp\left[-2\pi\lambda^s_{l,l} \sum_{j\in\mathcal{J}} \left\{ \int_{c_{i,j}(r,\theta^s_{\mathrm{t},l})}^{b_{i,j+1}(\theta^s_{\mathrm{t},l})} tp_{\mathrm{L}}(t) \left(1 - \frac{1}{\left(1 + \frac{z}{m_{\mathrm{L}}} P_t l_{\mathrm{L}}(t) G_j(t, \theta^s_{\mathrm{t},l})\right)^{m_{\mathrm{L}}}}\right) dt + \int_{c_{i,j}(r,\theta^s_{\mathrm{t},l})}^{b_{i,j+1}(\theta^s_{\mathrm{t},l})} tp_{\mathrm{N}}(t) \left(1 - \frac{1}{1 + z P_t l_{\mathrm{N}}(t) G_j(t, \theta^s_{\mathrm{t},l})}\right) dt \right\} \right] \quad (26)$$

Corollary 2: When the density of BSs approaches infinity (i.e., $\lambda_{\mathrm{B}} \to \infty$) and the optimal tilt angles are used for each scheme, the network outage probability of the ES-BS scheme is smaller than or equal to that of the IS-BS scheme, i.e.,

$$\mathcal{P}_{\mathrm{no}}^{\mathrm{IS}}\left(\theta_{\mathrm{t,O}}^{*}\right) \geq \mathcal{P}_{\mathrm{no}}^{\mathrm{ES}}\left(\theta_{\mathrm{t,G}}^{*}, \theta_{\mathrm{t,A}}^{*}\right). \tag{29}$$

Proof: When λ_{B} approaches infinity, $\lambda_{\mathrm{B,G}}^{s}$ and $\lambda_{\mathrm{B,A}}^{s}$ also approach infinity, respectively. Hence, in (19), regardless of the service provisioning scheme, the PDFs of the horizontal distance between the i-type user and the serving BS become similar, i.e., $f_{r_i^{vj}}(r) \approx f_{r_i^{vj}}^{\mathrm{IS},a}(r) \approx f_{r_i^{vj}}^{\mathrm{ES},a}(r)$. Substituting $f_{r_i^{vj}}(r)$ into (24) and using the optimal antenna tilt angles, network outage probabilities of i-type users for the IS-BS scheme and the ES-BS scheme, $\mathcal{P}_{\mathrm{no},i}^{\mathrm{IS}}(\theta_{\mathrm{t,O}}^{*})$ and $\mathcal{P}_{\mathrm{no},i}^{\mathrm{ES}}(\theta_{\mathrm{t},i}^{*})$, can be represented as

$$\begin{aligned}
\mathcal{P}_{\mathrm{no},i}^{\mathrm{IS}}(\theta_{\mathrm{t,O}}^{*}) &= \sum_{\substack{j\in\mathcal{J},\\ v\in\{\mathrm{L,N}\}}} \left(\int_{b_{i,j}(\theta_{\mathrm{t,O}}^{*})}^{b_{i,j+1}(\theta_{\mathrm{t,O}}^{*})} \mathcal{A}_{vj}^{a} \hat{\mathcal{P}}_{\mathrm{o},j}^{v}(r, \theta_{\mathrm{t,O}}^{*}) f_{r_i^{vj}}(r)\, dr \right), \\
\mathcal{P}_{\mathrm{no},i}^{\mathrm{ES}}(\theta_{\mathrm{t},i}^{*}) &= \sum_{\substack{j\in\mathcal{J},\\ v\in\{\mathrm{L,N}\}}} \left(\int_{b_{i,j}(\theta_{\mathrm{t},i}^{*})}^{b_{i,j+1}(\theta_{\mathrm{t},i}^{*})} \mathcal{A}_{vj}^{a} \hat{\mathcal{P}}_{\mathrm{o},j}^{v}(r, \theta_{\mathrm{t},i}^{*}) f_{r_i^{vj}}(r) dr \right).
\end{aligned} \tag{30}$$

In (30), we can always obtain $\mathcal{P}_{\mathrm{no},i}^{\mathrm{IS}}\left(\theta_{\mathrm{t,O}}^{*}\right) \geq \mathcal{P}_{\mathrm{no},i}^{\mathrm{ES}}\left(\theta_{\mathrm{t},i}^{*}\right)$, $\forall i \in \{\mathrm{G, A}\}$ because $\theta_{\mathrm{t,G}}^{*}$ and $\theta_{\mathrm{t,A}}^{*}$ in the ES-BS scheme are optimized ones for GUs and AUs, respectively, while in the IS-BS scheme, $\theta_{\mathrm{t,O}}^{*}$ is optimized one for both type users to minimize the total network outage probability. Therefore, from (23), we can conclude as (29). ■

From Corollary 2, we can see that when the density of BSs is sufficiently large, the ES-BS scheme outperforms the IS-BS scheme in terms of the network outage probability. Therefore, when the number of BSs is large enough, it is beneficial to exclusively serve GUs and AUs by independently optimizing the BS antenna tilt angles. This is also verified in Section IV, through the simulation results.

IV. NUMERICAL RESULTS

In this section, we evaluate the effect of the BS antenna tilt angle, the BS density, the interfering BS density, and the network parameters on the network outage probability. We first show the network outage probability on each of the IS-BS and ES-BS schemes. We then compare the performance of service provisioning schemes. In the numerical results, for the convenience of explanation, we denote the total interfering density as λ_{I} regardless of the scheme, i.e., $\lambda_{\mathrm{I}} = \lambda_{\mathrm{I,O}}^{\mathrm{IS}} = \lambda_{\mathrm{I,G}}^{\mathrm{ES}} + \lambda_{\mathrm{I,A}}^{\mathrm{ES}}$. Unless otherwise specified, we use the simulation parameters given in Table 2 based on the 3GPP specification and consider the dense urban environment parameters μ, ν and ξ [29], [39].

A. OUTAGE PROBABILITY OF GROUND AND AIR USERS

In this subsection, we analyze the impact of the BS antenna tilt angle on the outage probabilities of GUs and AUs.

TABLE 2. Environment parameters.

Parameters	Values	Parameters	Values
α_{L}	2.5	α_{N}	3.5
P_{t} [W]	3.5	σ^2 [W]	10^{-9}
μ	0.5	ν	3×10^{-4}
ξ	40	γ_{t}	1
m	3	h_{B} [m]	30
h_{G} [m]	0	h_{A} [m]	50
λ_{B} [BSs/m^2]	10^{-5}	ρ_{G}	0.5

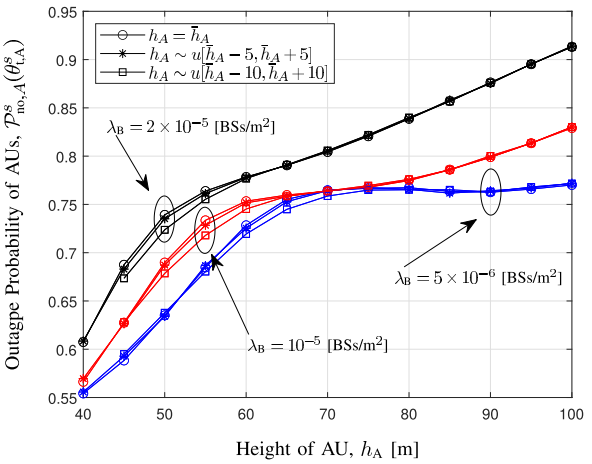

FIGURE 3. Outage probability of the AUs as a function of h_{A} for different AU height distributions and the BS density.

Figure 3 presents the outage probability of AUs for the cases of the fixed height $\bar{h}_A$ and the uniform distribution height (i.e., $h_{\mathrm{A}} \sim u[\bar{h}_A - \delta, \bar{h}_A + \delta]$). As shown in this figure, trends of the outage probability with the random height are similar to that with the fixed height only. Therefore, from this result, we show that only the performance of the fixed height case in the following figures. Even though there is a gap between the performance of the random height and that of the fixed height, the optimal height that minimizes the outage probability is almost the same.

Figure 4 presents the outage probability of i-type users, $\mathcal{P}_{\mathrm{no},i}^{s}(\theta_{\mathrm{t},i}^{s})$, as a function of the BS antenna tilt angle, $\theta_{\mathrm{t},i}^{s}$, for different values of the interfering BS density, λ_{I}. In this figure, simulation and analysis results are denoted by lines and asterisk marks, respectively. We can see that our analysis is well matched with the simulation results. Furthermore, the outage probability with the strongest association rule has a similar trend to that with the nearest association rule. The outage probability of the nearest association is always higher than that of the strongest association. Hence, in the following figures, we present the numerical results of the nearest association only.

From Fig. 4, for large λ_{I} (e.g., $\lambda_{\mathrm{I}} \geq 5 \times 10^{-6}$) and GUs ($i = \mathrm{G}$), we can see that as $\theta_{\mathrm{t},i}^{s}$ increases, $\mathcal{P}_{\mathrm{no},i}^{s}(\theta_{\mathrm{t},i}^{s})$ first

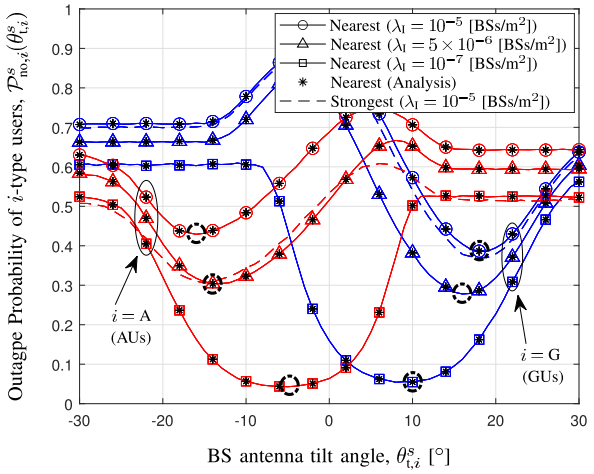

FIGURE 4. Outage probability of i-type users as a function of $\theta^s_{\mathrm{t},i}$ for different values of λ_I and BS association rules. The optimal BS antenna tilt angles, $\theta^*_{\mathrm{t},i}$, that minimize $\mathcal{P}^s_{\mathrm{no},i}(\theta^s_{\mathrm{t},i})$ are marked by dashed circles.

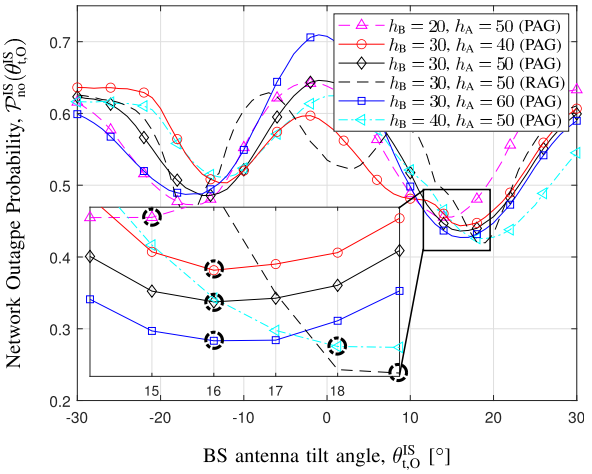

FIGURE 5. Network outage probability $\mathcal{P}^{\mathrm{IS}}_{\mathrm{no}}(\theta^{\mathrm{IS}}_{\mathrm{t,O}})$ as a function of $\theta^{\mathrm{IS}}_{\mathrm{t,O}}$ for different values of h_B and h_A with $\lambda_\mathrm{I} = 5 \times 10^{-6}$ [BSs/m^2]. The optimal BS antenna tilt angles, $\theta^*_{\mathrm{t,O}}$, that minimize $\mathcal{P}^{\mathrm{IS}}_{\mathrm{no}}(\theta^{\mathrm{IS}}_{\mathrm{t,O}})$ are marked by dashed circles.

increases up to a certain value of $\theta^s_{\mathrm{t},i}$, and then decreases. This is because as $\theta^s_{\mathrm{t},i}$ increases, the number of interfering BSs that form the antenna main lobe gain to the GU increases, i.e., the GU receives larger interference. However, for relatively large $\theta^s_{\mathrm{t},i}$ (e.g., $0° < \theta^s_{\mathrm{t},i} < 15°$), the serving BS can transmit the signal with the antenna main lobe gain to the GU mostly, while the number of interfering BSs with the antenna main lobe gain decreases. Therefore, $\mathcal{P}^s_{\mathrm{no},i}(\theta^s_{\mathrm{t},i})$ decreases with $\theta^s_{\mathrm{t},i}$. Furthermore, when $\theta^s_{\mathrm{t},i}$ is much large (e.g., $\theta^s_{\mathrm{t},i} > 20°$), as $\theta^s_{\mathrm{t},i}$ increases, the serving BS transmits the signal with the antenna side lobe gain to the GU with high probability. In this case, the performance loss of the main link is dominant, so $\mathcal{P}^s_{\mathrm{no},i}(\theta^s_{\mathrm{t},i})$ increases again. For AUs (i = A), the trend becomes the opposite, but the reason is the same as the case of GUs. For small λ_I (e.g., $\lambda_\mathrm{I} \leq 10^{-7}$), the main link channel's quality, which is affected by the antenna gain, mainly determines the performance. Hence, we observe that as $\theta^s_{\mathrm{t},i}$ increases, $\mathcal{P}^s_{\mathrm{no},i}(\theta^s_{\mathrm{t},i})$ first decreases and then increases. This is because as $\theta^s_{\mathrm{t},i}$ increases, the main lobe of the serving BS is first closer to the user, and then gets further away.

From Fig. 4, we can also see that as λ_I increases, the absolute value of the optimal tilt angle for i-type users, $\theta^*_{\mathrm{t},i}$, which is marked by the dashed circle in the figure, increases. This is to ensure that the number of interfering BSs with the antenna main lobe gain to the GU or AU decreases, as the number of interfering BSs increases.

B. RESULTS OF IS-BS SCHEME

In this subsection, we analyze the impact of the BS antenna tilt angle on the network outage probability with the IS-BS scheme.

Figure 5 presents the network outage probability of the IS-BS scheme, $\mathcal{P}^{\mathrm{IS}}_{\mathrm{no}}(\theta^{\mathrm{IS}}_{\mathrm{t,O}})$, as a function of the BS antenna tilt angle, $\theta^{\mathrm{IS}}_{\mathrm{t,O}}$, for different values of the BS height, h_B, and the AU height, h_A. Here, we use $\lambda_\mathrm{I} = 5 \times 10^{-6}$. In this figure, for $h_\mathrm{B} = 30$ and $h_\mathrm{A} = 50$, we compare the network outage probability with the rectangular antenna gain (RAG) model (i.e., the constant main lobe gain model) to the one in (23) that uses the parabolic antenna gain (PAG) model. We can see that the trend of the network outage probabilities with RAG and PAG models is different according to $\theta^{\mathrm{IS}}_{\mathrm{t,O}}$. Hence, the optimized antenna tilt angle with RAG model (i.e., $\theta^*_{\mathrm{t,O}} = 19°$) is not the one that minimizes the network outage probability for the PAG model (i.e., $\theta^*_{\mathrm{t,O}} = 16°$).

From Fig. 5, we can see that the optimal values of the BS antenna tilt angle, $\theta^*_{\mathrm{t,O}}$, exist in the considerably down tilted regions. As shown in Fig. 4, the difference of the optimal antenna tilt angles for GUs and AUs increases as λ_I increases. Consequently, in terms of the network performance of the IS-BS scheme, it is worth optimizing the antenna tilt angle toward certain types of users, i.e., GUs or AUs. Specifically, for a given configuration, AUs are more affected by interference due to high LoS probability than GUs, hence BSs transmit the signal to AUs with the side lobe to reduce interfering signal power. On the other hand, to increase the main link power, BSs transmit the signal to GUs with the main lobe. Therefore, to minimize network outage probability, the BS antenna needs to be tilted downwards.

We can also see that for the fixed height of AUs (e.g., $h_\mathrm{A} = 50$ m), as the height of the BS increases (e.g., $h_\mathrm{B} = 20 \sim 40$ m), the optimal value of the BS antenna tilt angle increases. This is to reduce the number of interfering BSs which has the antenna main lobe gain to GUs and ensure that most serving BS transmits the signal with the antenna main lobe gain to GUs. On the contrary, for the fixed height of BSs (e.g., $h_\mathrm{B} = 30$ m), there is no change in the optimal tilt angle according to h_A, because AUs are served by the side lobe.

Figure 6 presents the optimal value of the BS antenna tilt angle, $\theta^*_{\mathrm{t,O}}$, according to the ratio of GUs to total users, ρ_G, for different values of the total BS density, λ_B, with the IS-BS scheme. Here, we use $\lambda_\mathrm{I} = 0.1\lambda_\mathrm{B}$. From Fig. 6, we can see

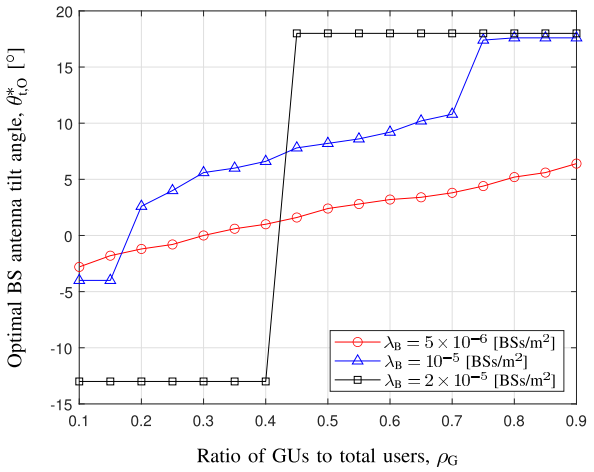

FIGURE 6. Optimal BS antenna tilt angle, $\theta^*_{t,O}$, according to ρ_G for different values of λ_B in the IS-BS scheme.

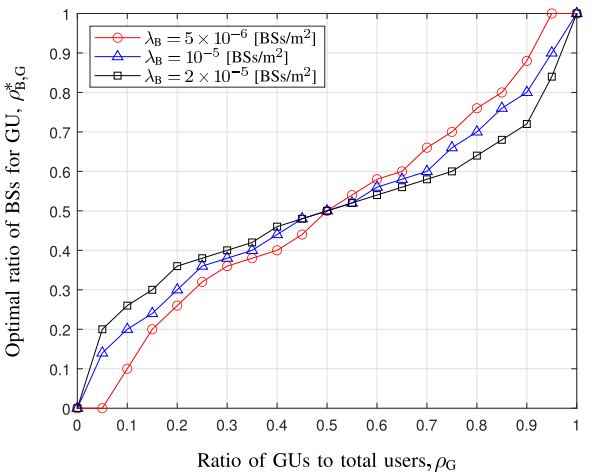

FIGURE 7. Optimal ratio of BSs for GUs to total BS $\rho_{B,G}$ according to ρ_G for different values of λ_B in the ES-BS scheme.

that as ρ_G increases, the optimal value of the BS antenna tilt angle, $\theta^*_{t,O}$, also increases. Since the interference is not significant in this environment, the main link channel's quality mainly determines the network performance dominantly. Hence, as the portion of GUs increases, the BS needs to tilt its antenna downward. For large λ_B (e.g., $\lambda_B \geq 2 \times 10^{-5}$), we can also observe that the optimal antenna tilt angle is either downwards (e.g., $\theta^*_{t,O} = 18°$) or upwards (e.g., $\theta^*_{t,O} = -13°$). Because of the significant difference of the optimal antenna tilt angles for GUs and AUs, it is worth optimizing the antenna tilt angle toward certain types of users, as also explained in Fig. 5.

C. RESULTS OF ES-BS SCHEME

In this subsection, we analyze the impact of the BS antenna tilt angle on the network outage probability with the ES-BS scheme. Note that, in the ES-BS scheme, since the GUs and AUs are exclusively served by the BSs, the antenna tilt angles for GUs, $\theta^{ES}_{t,G}$, and AUs, $\theta^{ES}_{t,A}$, are independently designed to minimize the network outage probability. Furthermore, in the ES-BS scheme, the ratio of GBSs affects the optimal BS tilt angles, and hence we optimize BS tilt angles in accordance with the ratio of GBSs to total BSs, $\rho_{B,G}$.

Figure 7 shows the optimal ratio of GBSs to total BSs, $\rho^*_{B,G}$, that minimizes the network outage probability, according to the GU ratio to total users, ρ_G. We consider different values of the total BS density, λ_B, and we use $\lambda_I = 0.1\lambda_B$. In Fig. 7, as ρ_G increases, $\rho^*_{B,G}$ also increases. This is because it is beneficial to have more GBSs when the portion of GUs is large. We can also see that for large ρ_G (e.g., $\rho_G > 0.5$), $\rho^*_{B,G}$ decreases as λ_B increases. This is because there is more the number of BSs, so we can have enough GBSs with small $\rho^*_{B,G}$. Thus, we can assign a larger portion of BSs as the ABSs. On the contrary, when ρ_G is small (e.g., $\rho_G < 0.5$), $\rho^*_{B,G}$ increases as λ_B increases for a similar reason.

Figure 8 presents the optimal value of the BS antenna tilt angles, $\theta^*_{t,G}$ and $\theta^*_{t,A}$, according to the ratio of GUs to total

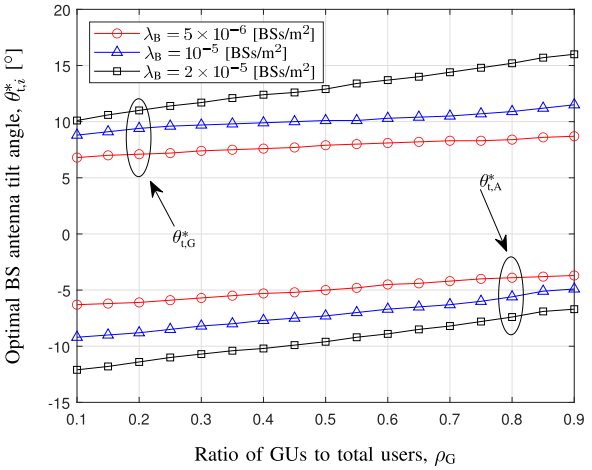

FIGURE 8. Optimal BS antenna tilt angle ($\theta^*_{t,G}$, and $\theta^*_{t,A}$) according to ρ_G for different values of λ_B in the ES-BS scheme.

users, ρ_G, for different values of the total BS density, λ_B, with ES-BS scheme. Here, we use $\lambda_I = 0.1\lambda_B$. From Fig. 8, we can see that as ρ_G increases, $\theta^*_{t,G}$ and $\theta^*_{t,A}$ also increase. In the ES-BS scheme, as ρ_G increases $\rho^*_{B,G}$ also increases, as shown in Fig. 7. Therefore, as the number of BSs increases, to reduce the number of interfering BSs giving the large interference with the antenna main lobe gain, the antenna is tilted more downwards or upwards. For the same reason, we can observe that for given ρ_G, as λ_B increases, the absolute values of $\theta^*_{t,G}$ and $\theta^*_{t,A}$ also increase.

D. COMPARISON BETWEEN IS-BS SCHEME AND ES-BS SCHEME

In this subsection, we compare the performance of the BS service provisioning schemes in terms of the network outage probability according to the ratio of GUs to total users, ρ_G. For the comparison of the IS-BS scheme and the ES-BS scheme, the antenna tilt angle of the IS-BS scheme ($\theta^{IS}_{t,O}$), that

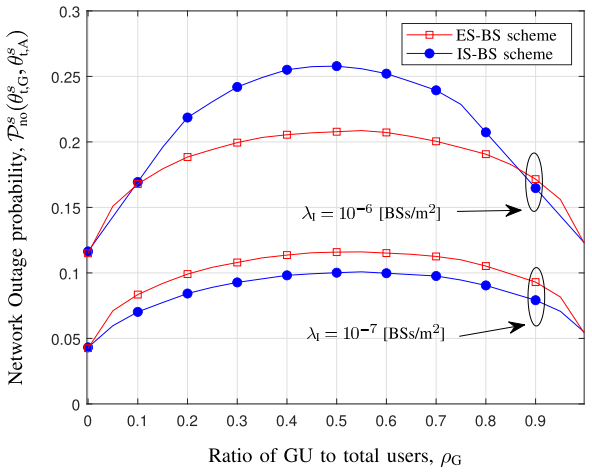

FIGURE 9. Network outage probability of the IS-BS and ES-BS schemes according to ρ_G with different values of λ_I.

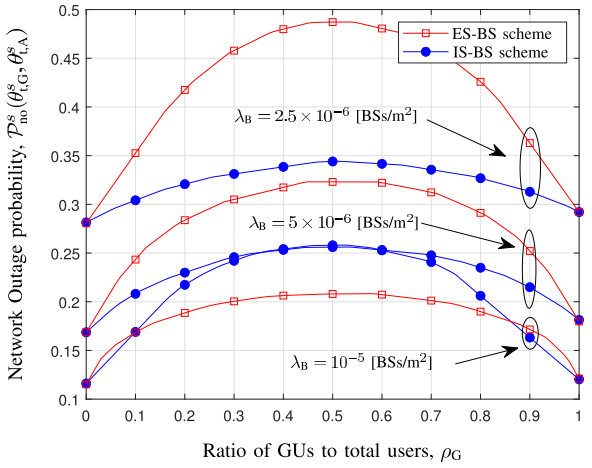

FIGURE 10. Network outage probability of the IS-BS and ES-BS schemes according to ρ_G with different values of λ_B.

of the ES-BS scheme ($\theta_{t,G}^{ES}$, $\theta_{t,A}^{ES}$), and the ratio of GBSs ($\rho_{B,G}$) are optimized, respectively.

Figure 9 presents the network outage probability, $\mathcal{P}_{no}^{s}(\theta_{t,G}^{s}, \theta_{t,A}^{s})$, as a function of the ratio of GUs, ρ_G, for different values of λ_I and service provisioning schemes. From Fig. 9, we can see that when λ_I is large (e.g., $\lambda_I \geq 10^{-6}$), the ES-BS scheme outperforms the IS-BS scheme. This is because, for the ES-BS scheme, interfering BSs of different types from the serving BS mostly transmit signals to the user with antenna side lobe gain. On the other hand, for small λ_I (e.g., $\lambda_I \leq 10^{-7}$), the IS-BS scheme performs better than the ES-BS scheme. This is because the effect of the interference is relatively small, so more serving BS candidates (i.e., $\lambda_{B,i}^{IS} > \lambda_{B,i}^{ES}$) can improve the performance of the main link.

Figure 10 presents the network outage probability, $\mathcal{P}_{no}^{s}(\theta_{t,G}^{s}, \theta_{t,A}^{s})$, as a function of the ratio of GUs ρ_G for different values of the total BS density λ_B and different service provisioning schemes. Here, we use $\lambda_I = 0.1\lambda_B$. From Fig. 10, we can see that when the total BS density is

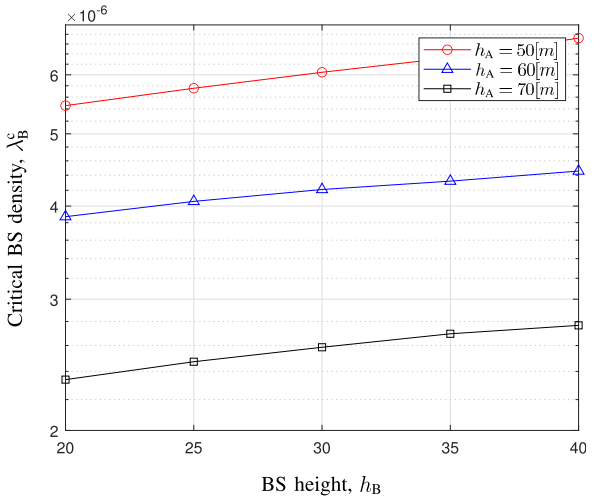

FIGURE 11. Critical BS density λ_B^c according to h_B with different values h_A.

small (e.g., $\lambda_B \leq 5 \times 10^{-6}$), the IS-BS scheme outperforms the ES-BS scheme. On the contrary, for the large total BS density (e.g., $\lambda_B \geq 10^{-5}$), the ES-BS scheme provides better performance than the IS-BS scheme in terms of the network outage probability. From these observations, we can find that when there exist enough BSs in the network, it is beneficial to exclusively serve each type of user by independently optimizing the BS antenna tilt angle for each type of user (ES-BS scheme). On the other hand, when the number of BSs is relatively small, the efficient service provisioning scheme is that all BSs serve both GUs and AUs by optimizing the BS antenna tilt angle to maximize the network performance (IS-BS scheme).

In Corollary 2 and Fig. 10, for large λ_B, the ES-BS scheme outperforms the IS-BS scheme, and for small λ_B, vice versa. Therefore, there exist the value of λ_B that makes the performance of the two schemes to be equal such as $\mathcal{P}_{no}^{IS}(\theta_{t,O}^{IS}) = \mathcal{P}_{no}^{ES}(\theta_{t,G}^{ES}, \theta_{t,A}^{ES})$, and we define this value of λ_B as the *critical density of BSs*, λ_B^c. That means in the region of $\lambda_B < \lambda_B^c$, the IS-BS scheme is superior to the ES-BS scheme in terms of the network outage probability and vice versa.

Figure 11 presents the critical density of the BSs, λ_B^c, as a function of the BS height, h_B, for the different values of the AU height, h_A. In this figure, we can see that as the distance between the BS and the AU becomes closer, (i.e., h_B increases for fixed h_A or h_A decreases for fixed h_B), λ_B^c increases. In this case, since the performance of the AUs is good enough due to the relatively short distance, the BS in the IS-BS scheme mainly tilt the antenna for GUs to enhance the network performance. Therefore, the IS-BS scheme can provide better performance than the ES-BS scheme. In contrast, for the case that the BS is far from the AUs, the BS in the IS-BS scheme has to properly tilt the antenna by considering the performance of both GU and AU. Therefore, in this case, the ES-BS scheme can be more efficient as it can be independently optimized the antenna tilt angles for GUs and AUs, respectively.

V. CONCLUSION

This paper explores an appropriate BS service provisioning scheme to serve both GUs and AUs by considering tilt angle-based antenna gain. We first derive the network outage probability for two types of provisioning schemes, i.e., IS-BS scheme and ES-BS scheme (in Theorem 1). We then explore the conflict impact of the antenna tilt angle on the network outage probability, i.e., as the absolute value of the tilt angle decreases, the main lobe service area becomes wider, but the main link distance increases (in Corollary 1 and Remark 1). From this relation, we numerically show that there exists the optimal BS antenna tilt angle that minimizes the network outage probability. Moreover, we show the impact of the ratio of GUs, the BS height, the UAV height, and densities of the total BSs and the interfering BSs on the optimal tilt angle as well as network outage probabilities for two service provisioning schemes. Finally, for given network parameters, we present which service provisioning scheme is more appropriate. Specifically, in Corollary 2, we show that the ES-BS scheme is better than the IS-BS scheme when BSs are densely deployed. In contrast, the IS-BS scheme performs better than the ES-BS scheme for low BS density or interfering BS density. The outcomes of this work can be useful for the optimal antenna tilt angle design and the BS provisioning service scheme determination in the networks, where both GUs and AUs exist.

APPENDIX

PROOF OF THEOREM 1

From (20) and (22), $\mathcal{P}^{v}_{\mathrm{o},j}(r^{vj}_{k,\mathbf{x}_\tau}, \theta^{s}_{\mathrm{t},i})$ can be presented by

$$\begin{aligned}
&\mathcal{P}^{v}_{\mathrm{o},j}(r^{vj}_{k,\mathbf{x}_\tau}, \theta^{s}_{\mathrm{t},i}) \\
&= \mathbb{P}\left[\Omega_{k,\mathbf{x}_\tau} < \frac{\gamma_{\mathrm{t}}(I^s+\sigma^2)}{P_{\mathrm{t}} l_v\left(r^{vj}_{k,\mathbf{x}_\tau}\right) G_j(r^{vj}_{k,\mathbf{x}_\tau}, \theta^{s}_{\mathrm{t},i})}\right] \\
&\overset{(a)}{=} \mathbb{E}_{I^s}\left[\frac{\gamma\left(m_v, \frac{m_v\gamma_{\mathrm{t}}(I^s+\sigma^2)}{P_{\mathrm{t}} l_v\left(r^{vj}_{k,\mathbf{x}_\tau}\right) G_j(r^{vj}_{k,\mathbf{x}_\tau}, \theta^{s}_{\mathrm{t},i})}\right)}{\Gamma(m_v)}\right] \\
&\overset{(b)}{=} 1 - \mathbb{E}_{I^s}\left[\sum_{n=0}^{m_v-1}\frac{1}{n!}\left(\frac{m_v\gamma_{\mathrm{t}}(I^s+\sigma^2)}{P_{\mathrm{t}} l_v\left(r^{vj}_{k,\mathbf{x}_\tau}\right) G_j(r^{vj}_{k,\mathbf{x}_\tau}, \theta^{s}_{\mathrm{t},i})}\right)^n \right. \\
&\qquad \left. \times \exp\left(-\frac{m_v\gamma_{\mathrm{t}}(I^s+\sigma^2)}{P_{\mathrm{t}} l_v\left(r^{vj}_{k,\mathbf{x}_\tau}\right) G_j(r^{vj}_{k,\mathbf{x}_\tau}, \theta^{s}_{\mathrm{t},i})}\right)\right],
\end{aligned} \tag{31}$$

where (a) is from the CDF of the Gamma distribution, and (b) follows from the definition of the incomplete gamma function for integer values of m_v. From (31), we obtain (25) by using $\mathbb{E}_{I^s}[\exp(-z(I^s+\sigma^2))] = \mathcal{L}_{I^s}(z)\exp(-z\sigma^2)$ and following property

$$\mathbb{E}_{I^s}[(-I^s)^n \exp(-zI^s)] = \frac{d}{dz^n}\mathcal{L}_{I^s}(z). \tag{32}$$

In (25), $\mathcal{L}_{I^{\mathrm{IS}}}(z) = \mathcal{L}_{I^{\mathrm{IS}}_0}(z)$ and $\mathcal{L}_{I^{\mathrm{ES}}}(z) = \mathcal{L}_{I^{\mathrm{ES}}_{\mathrm{G}}}(z)\mathcal{L}_{I^{\mathrm{ES}}_{\mathrm{A}}}(z)$, and $\mathcal{L}_{I^s_l}(z)$, $l \in \{\mathrm{O},\mathrm{G},\mathrm{A}\}$, is given by

$$\begin{aligned}
&\mathcal{L}_{I^s_l}(z) \\
&= \mathbb{E}_{\Phi_{\mathrm{I},l}}\left[\exp\left(-z\sum_{\mathbf{x}\in\Phi_{\mathrm{I},l}\setminus\{\mathbf{x}_\tau\}} P_{\mathrm{t}}\Omega_{k,\mathbf{x}} l_v\left(r_{k,\mathbf{x}}\right) G_j(r_{k,\mathbf{x}}, \theta^{s}_{\mathrm{t},l})\right)\right] \\
&= \mathbb{E}_{\Phi_{\mathrm{I},l}}\left[\prod_{\mathbf{x}\in\Phi_{\mathrm{I},l}\setminus\{\mathbf{x}_\tau\}} \mathbb{E}_{\Omega_{k,\mathbf{x}}}\left[\exp\left\{-zP_{\mathrm{t}}\Omega_{k,\mathbf{x}} l_v\left(r_{k,\mathbf{x}}\right) G_j(r_{k,\mathbf{x}}, \theta^{s}_{\mathrm{t},l})\right\}\right]\right] \\
&\overset{(a)}{=} \mathbb{E}_{\Phi_{\mathrm{I},l}}\left[\prod_{\mathbf{x}\in\Phi_{\mathrm{I},l}\setminus\{\mathbf{x}_\tau\}} \left\{\frac{p_{\mathrm{L}}\left(r_{k,\mathbf{x}}\right)}{\left(1+\frac{z}{m_{\mathrm{L}}}P_{\mathrm{t}} l_{\mathrm{L}}(r_{k,\mathbf{x}}) G_j(r_{k,\mathbf{x}}, \theta^{s}_{\mathrm{t},l})\right)^{m_{\mathrm{L}}}}\right.\right. \\
&\qquad \left.\left. + \frac{p_{\mathrm{N}}\left(r_{k,\mathbf{x}}\right)}{1+zP_{\mathrm{t}} l_{\mathrm{N}}(r_{k,\mathbf{x}}) G_j(r_{k,\mathbf{x}}, \theta^{s}_{\mathrm{t},l})}\right\}\right],
\end{aligned} \tag{33}$$

where $\mathbf{x}_\tau$ is the location of the serving BS, and (a) is from the Laplace transforms of the Gamma distribution and the exponential distribution. From (33), by applying the probability generating functional (PGFL) [40], we obtain (26).

By averaging $\mathcal{P}^{v}_{\mathrm{o},j}(r^{vj}_{k,\mathbf{x}_\tau}, \theta^{s}_{\mathrm{t},i})$ in (25) over $r^{vj}_{k,\mathbf{x}_\tau}$, $\mathcal{P}^{s}_{\mathrm{no},i}(\theta^{s}_{\mathrm{t},i})$ is given by

$$\begin{aligned}
\mathcal{P}^{s}_{\mathrm{no},i}(\theta^{s}_{\mathrm{t},i}) &= \mathbb{E}_{r^{vj}_{k,\mathbf{x}_\tau}}\left[\mathcal{P}^{v}_{\mathrm{o},j}(r^{vj}_{k,\mathbf{x}_\tau}, \theta^{s}_{\mathrm{t},i})\right] \\
&\overset{(a)}{=} \sum_{\substack{j\in\mathcal{J},\\ v\in\{\mathrm{L},\mathrm{N}\}}}\left(\int_{b_{k,j}(\theta^{s}_{\mathrm{t},i})}^{b_{k,j+1}(\theta^{s}_{\mathrm{t},i})} \mathcal{A}^{a}_{vj}\mathcal{P}^{v}_{\mathrm{o},j}(r, \theta^{s}_{\mathrm{t},i}) f^{s,a}_{r^{vj}_{k,\mathbf{x}_\tau}}(r)dr\right),
\end{aligned} \tag{34}$$

where (a) is from the definition of $\Phi^{vj}_{\mathrm{B},l}$ in (12). In (34), for $k \in \mathcal{U}_i$, by substituting from $f^{s,a}_{r^{vj}_{k,\mathbf{x}_\tau}}(r)$ and $b_{k,j}(\theta^{s}_{\mathrm{t},i})$ to $f^{s,a}_{r^{vj}_{i}}(r)$ and $b_{i,j}(\theta^{s}_{\mathrm{t},i})$, respectively, we obtain (24). Finally, using the law of total probability and (24), the network outage probability for the given ratio of GUs and AUs, ρ_{G} and ρ_{A}, is given in (23).

ACKNOWLEDGMENT

Any opinions, findings and conclusions or recommendations expressed in this material are those of the author(s) and do not reflect the views of National Research Foundation, Singapore, and Infocomm Media Development Authority.

An earlier version of this paper was presented in part at the IEEE Global Communications Conference, Taipei, Taiwan, December 2020 [41] [DOI: 10.1109/GLOBECOM42002.2020.9322137].

REFERENCES

[1] F. Rinaldi, H.-L. Maattanen, J. Torsner, S. Pizzi, S. Andreev, A. Iera, Y. Koucheryavy, and G. Araniti, "Non-terrestrial networks in 5G & beyond: A survey," *IEEE Access*, vol. 8, pp. 165178–165200, 2020.

[2] M. Giordani and M. Zorzi, "Non-terrestrial networks in the 6G era: Challenges and opportunities," *IEEE Netw.*, vol. 35, no. 2, pp. 244–251, Mar. 2021.

[3] X. Lin, S. Rommer, S. Euler, E. A. Yavuz, and R. S. Karlsson, "5G from space: An overview of 3GPP non-terrestrial networks," 2021, *arXiv:2103.09156*.

[4] Y. Zeng, R. Zhang, and T. J. Lim, "Wireless communications with unmanned aerial vehicles: Opportunities and challenges," *IEEE Commun. Mag.*, vol. 54, no. 5, pp. 36–42, May 2016.
[5] N. H. Motlagh, M. Bagaa, and T. Taleb, "UAV-based IoT platform: A crowd surveillance use case," *IEEE Commun. Mag.*, vol. 55, no. 2, pp. 128–134, Feb. 2017.
[6] S. Hayat, E. Yanmaz, and R. Muzaffar, "Survey on unmanned aerial vehicle networks for civil applications: A communications viewpoint," *IEEE Commun. Surveys Tuts.*, vol. 18, no. 4, pp. 2624–2661, 4th Quart., 2016.
[7] A. A. Khuwaja, Y. Chen, N. Zhao, M.-S. Alouini, and P. Dobbins, "A survey of channel modeling for UAV communications," *IEEE Commun. Surveys Tuts.*, vol. 20, no. 4, pp. 2804–2821, 4th Quart., 2018.
[8] A. Al-Hourani and K. Gomez, "Modeling cellular-to-UAV path-loss for suburban environments," *IEEE Wireless Commun. Lett.*, vol. 7, no. 1, pp. 82–85, Feb. 2018.
[9] A. Al-Hourani, S. Kandeepan, and S. Lardner, "Optimal LAP altitude for maximum coverage," *IEEE Wireless Commun. Lett.*, vol. 3, no. 6, pp. 569–572, Dec. 2014.
[10] H. Cho, C. Liu, J. Lee, T. Noh, and T. Q. S. Quek, "Impact of elevated base stations on the ultra-dense networks," *IEEE Commun. Lett.*, vol. 22, no. 6, pp. 1268–1271, Jun. 2018.
[11] M. M. Azari, F. Rosas, K.-C. Chen, and S. Pollin, "Ultra reliable UAV communication using altitude and cooperation diversity," *IEEE Trans. Commun.*, vol. 66, no. 1, pp. 330–344, Jan. 2018.
[12] P. K. Sharma and D. I. Kim, "UAV-enabled downlink wireless system with non-orthogonal multiple access," in *Proc. IEEE Globecom Workshops (GC Wkshps)*, Dec. 2017, pp. 1–6.
[13] H. He, S. Zhang, Y. Zeng, and R. Zhang, "Joint altitude and beamwidth optimization for UAV-enabled multiuser communications," *IEEE Commun. Lett.*, vol. 22, no. 2, pp. 344–347, Feb. 2018.
[14] M. Mozaffari, W. Saad, M. Bennis, and M. Debbah, "Efficient deployment of multiple unmanned aerial vehicles for optimal wireless coverage," *IEEE Commun. Lett.*, vol. 20, no. 8, pp. 1647–1650, Aug. 2016.
[15] J. Lyu, Y. Zeng, and R. Zhang, "UAV-aided offloading for cellular hotspot," *IEEE Trans. Wireless Commun.*, vol. 17, no. 6, pp. 3988–4001, Jun. 2018.
[16] S. Zhang, Y. Zeng, and R. Zhang, "Cellular-enabled UAV communication: A connectivity-constrained trajectory optimization perspective," *IEEE Trans. Commun.*, vol. 67, no. 3, pp. 2580–2604, Mar. 2019.
[17] M. Kim and J. Lee, "Impact of an interfering node on unmanned aerial vehicle communications," *IEEE Trans. Veh. Technol.*, vol. 68, no. 12, pp. 12150–12163, Dec. 2019.
[18] D. Kim, J. Lee, and T. Q. S. Quek, "Multi-layer unmanned aerial vehicle networks: Modeling and performance analysis," *IEEE Trans. Wireless Commun.*, vol. 19, no. 1, pp. 325–339, Jan. 2020.
[19] Y. Zeng, J. Lyu, and R. Zhang, "Cellular-connected UAV: Potential, challenges, and promising technologies," *IEEE Wireless Commun.*, vol. 26, no. 1, pp. 120–127, Feb. 2019.
[20] X. Lin and V. Yajnanarayana, "The sky is not the limit: LTE for unmanned aerial vehicles," *IEEE Commun. Mag.*, vol. 56, no. 4, pp. 204–210, Apr. 2018.
[21] B. Galkin, J. Kibilda, and L. A. DaSilva, "Backhaul for low-altitude UAVs in urban environments," in *Proc. IEEE Int. Conf. Commun. (ICC)*, Kansas City, MO, USA, May 2018, pp. 1–6.
[22] M. M. Azari, F. Rosas, A. Chiumento, and S. Pollin, "Coexistence of terrestrial and aerial users in cellular networks," in *Proc. IEEE Globecom Workshops (GC Wkshps)*, Singapore, Dec. 2017, pp. 1–6.
[23] M. M. Azari, F. Rosas, and S. Pollin, "Reshaping cellular networks for the sky: Major factors and feasibility," in *Proc. IEEE Int. Conf. Commun. (ICC)*, Kansas City, MO, USA, May 2018, pp. 1–7.
[24] R. Amer, W. Saad, and N. Marchetti, "Toward a connected sky: Performance of beamforming with down-tilted antennas for ground and UAV user co-existence," *IEEE Commun. Lett.*, vol. 23, no. 10, pp. 1840–1844, Oct. 2019.
[25] X. Xu and Y. Zeng, "Cellular-connected UAV: Performance analysis with 3D antenna modelling," in *Proc. IEEE Int. Conf. Commun. Workshops (ICC Workshops)*, Shanghai, China, May 2019, pp. 1–6.
[26] R. Amer, W. Saad, B. Galkin, and N. Marchetti, "Performance analysis of mobile cellular-connected drones under practical antenna configurations," in *Proc. IEEE Int. Conf. Commun. (ICC)*, Dublin, Ireland, Jun. 2020, pp. 1–7.
[27] R. Amer, W. Saad, and N. Marchetti, "Mobility in the sky: Performance and mobility analysis for cellular-connected UAVs," *IEEE Trans. Commun.*, vol. 68, no. 5, pp. 3229–3246, May 2020.
[28] *Technical Specification Group Radio Access Network: Evolved Universal Terrestrial Radio Access (E-UTRA): Further Advancements for E-UTRA Physical Layer Aspects*, document TR 36.814 V9.2.0, Tech. Rep., Mar. 2017.
[29] *Technical Specification Group Radio Access Network: Study on Enhanced LTE Support for Aerial Vehicles*, document TR 36.777 V15.0.0, Dec. 2017.
[30] Y. Zhu, G. Zheng, and M. Fitch, "Secrecy rate analysis of UAV-enabled mmWave networks using Matérn hardcore point processes," *IEEE J. Sel. Areas Commun.*, vol. 36, no. 7, pp. 1397–1409, Jul. 2018.
[31] J. Lyu and H.-M. Wang, "Secure UAV random networks with minimum safety distance," *IEEE Trans. Veh. Technol.*, vol. 70, no. 3, pp. 2856–2861, Mar. 2021.
[32] Z. Yang, L. Zhou, G. Zhao, and S. Zhou, "Blockage modeling for inter-layer UAVs communications in urban environments," in *Proc. 25th Int. Conf. Telecommun. (ICT)*, St. Malo, France, Jun. 2018, pp. 307–311.
[33] R. Hernandez-Aquino, S. A. R. Zaidi, D. McLernon, M. Ghogho, and A. Imran, "Tilt angle optimization in two-tier cellular networks—A stochastic geometry approach," *IEEE Trans. Commun.*, vol. 63, no. 12, pp. 5162–5177, Dec. 2015.
[34] S. M. Razavizadeh, M. Ahn, and I. Lee, "Three-dimensional beamforming: A new enabling technology for 5G wireless networks," *IEEE Signal Process. Mag.*, vol. 31, no. 6, pp. 94–101, Nov. 2014.
[35] M. Alzenad and H. Yanikomeroglu, "Coverage and rate analysis for unmanned aerial vehicle base stations with LoS/NLoS propagation," in *Proc. IEEE Globecom Workshops (GC Wkshps)*, Abu Dhabi, United Arab Emirates, Dec. 2018, pp. 1–7.
[36] F. Baccelli and B. Błaszczyszyn, "Stochastic geometry and wireless networks: Volume II- applications," *Found. Trends Netw.*, vol. 4, nos. 1–2, pp. 1–312, 2009, doi: 10.1561/1300000026.
[37] H. ElSawy, A. Sultan-Salem, M. S. Alouini, and M. Z. Win, "Modeling and analysis of cellular networks using stochastic geometry: A tutorial," *IEEE Commun. Surveys Tuts.*, vol. 19, no. 1, pp. 167–203, 1st Quart., 2017.
[38] S. S. Ikki and M. H. Ahmed, "Performance analysis of decode-and-forward incremental relaying cooperative-diversity networks over Rayleigh fading channels," in *VTC Spring - IEEE 69th Veh. Technol. Conf.*, Barcelona, Spain, Apr. 2009, pp. 1–6, doi: 10.1109/VETECS.2009.5073777.
[39] J. Holis and P. Pechac, "Elevation dependent shadowing model for mobile communications via high altitude platforms in built-up areas," *IEEE Trans. Antennas Propag.*, vol. 56, no. 4, pp. 1078–1084, Apr. 2008.
[40] M. Haenggi and R. K. Ganti, "Interference in large wireless networks," *Found. Trends Netw.*, vol. 3, no. 2, pp. 127–248, 2009.
[41] S. Kim, M. Kim, J. Y. Ryu, and J. Lee, "Impact of base station antenna tilt angle on UAV communications," in *Proc. IEEE Global Commun. Conf. (GLOBECOM)*, Taipei, Taiwan, Dec. 2020, pp. 1–6.

SEONGJUN KIM (Student Member, IEEE) received the B.S. degree from Kyungpook National University, Daegu, South Korea, in 2018. He is currently pursuing the Ph.D. degree with the Department of Electrical Engineering and Computer Science, Daegu Gyeongbuk Institute of Science and Technology (DGIST), Daegu. His research interests include the unmanned aerial vehicle communications and integrated access and backhaul networks.

MINSU KIM (Student Member, IEEE) received the B.S. degree in electrical engineering from Kookmin University, Seoul, South Korea, in 2017, and the M.S. degree from the Department of Electrical Engineering and Computer Science, Daegu Gyeongbuk Institute of Science and Technology (DGIST), Daegu, South Korea, in 2019, where he is currently pursuing the Ph.D. degree. His current research interests include multi-user multiple-input single-output networks, unmanned aerial vehicle communications, wireless security, and intelligent networking. He received the KICS Outstanding Paper Award in 2017.

JONG YEOL RYU (Member, IEEE) received the B.E. degree in electrical engineering from Chungnam National University, Daejeon, South Korea, in 2008, and the M.S. and Ph.D. degrees in electrical engineering from the Korea Advance Institute of Science and Technology, Daejeon, in 2010 and 2014, respectively. From 2014 to 2016, he was a Postdoctoral Fellow with the Singapore University of Technology and Design. He is currently an Associate Professor with the Department of Information and Communication Engineering, Gyeongsang National University, Tongyeong, South Korea. His current research interests include cell-free massive MIMO communications, physical layer security, and social aware communication systems.

JEMIN LEE (Member, IEEE) received the B.S. (Hons.), M.S., and Ph.D. degrees in electrical and electronic engineering from Yonsei University, Seoul, South Korea, in 2004, 2007, and 2010, respectively.

She was a Postdoctoral Fellow at the Massachusetts Institute of Technology (MIT), Cambridge, MA, USA, from 2010 to 2013, a Temasek Research Fellow at iTrust, Centre for Research in Cyber Security, Singapore University of Technology and Design (SUTD), Singapore, from 2014 to 2016, and an Associate Professor at the Department of Information and Communication Engineering, Daegu Gyeongbuk Institute of Science and Technology (DGIST), Daegu, South Korea, from 2016 to 2021. She is currently an Associate Professor at the Department of Electrical and Computer Engineering, Sungkyunkwan University (SKKU), Suwon, South Korea. Her current research interests include wireless communications, wireless security, intelligent networking, and blockchain networks. She received the Haedong Young Engineering Researcher Award in 2020, the IEEE ComSoc Young Author Best Paper Award in 2020, the IEEE ComSoc AP Outstanding Paper Award in 2017, the IEEE ComSoc AP Outstanding Young Researcher Award in 2014, the Temasek Research Fellowship in 2013, and the Chun-Gang Outstanding Research Award in 2011. She serves as a Chair for the IEEE Communication Society (ComSoc) Radio Communications Technical Committee (RCC). She has been serving as a Symposium/Track Chairs for a number of international conferences, including 2020 IEEE GLOBECOM and 2020 IEEE WCNC. She is also an Editor of the IEEE Wireless Communications Letters, and was an Editor of the IEEE Transactions on Wireless Communications and the IEEE Communication Letters, from 2014 to 2019.

TONY Q. S. QUEK (Fellow, IEEE) received the B.E. and M.E. degrees in electrical and electronics engineering from the Tokyo Institute of Technology, in 1998 and 2000, respectively, and the Ph.D. degree in electrical engineering and computer science from the Massachusetts Institute of Technology, in 2008.

He is currently the Cheng Tsang Man Chair Professor with the Singapore University of Technology and Design (SUTD). He also works as the Director of the Future Communications Research and Development Program, the Head of ISTD Pillar, and the Deputy Director of the SUTD-ZJU IDEA. His current research interests include wireless communications and networking, network intelligence, the Internet of Things, URLLC, and 6G.

Dr. Quek was honored with the 2008 Philip Yeo Prize for Outstanding Achievement in Research, the 2012 IEEE William R. Bennett Prize, the 2015 SUTD Outstanding Education Awards—Excellence in Research, the 2016 IEEE Signal Processing Society Young Author Best Paper Award, the 2017 CTTC Early Achievement Award, the 2017 IEEE ComSoc AP Outstanding Paper Award, the 2020 IEEE Communications Society Young Author Best Paper Award, the 2020 IEEE Stephen O. Rice Prize, the 2020 Nokia Visiting Professor, and the 2016–2020 Clarivate Analytics Highly Cited Researcher. He has been actively involved in organizing and chairing sessions, and has served as a member for the technical program committee as well as symposium chairs for a number of international conferences. He is also serving as an Area Editor for the IEEE Transactions on Wireless Communications and an Elected Member of the IEEE Signal Processing Society SPCOM Technical Committee. He was an Executive Editorial Committee Member of the IEEE Transactions on Wireless Communications, an Editor of the IEEE Transactions on Communications, and an Editor of the IEEE Wireless Communications Letters.